



UNIVERSITAT POLITÈCNICA
DE CATALUNYA
BARCELONATECH



INSTRUMENTATION, SENSORS
AND INTERFACES GROUP

Escola Tècnica Superior d'Enginyeria de Telecomunicació de Barcelona

Physics Engineering Degree

Final Degree Project in Physics Engineering

Outpatient system for multipoint monitoring of the IPG signal

Josep Maria Ferrer Sánchez

Thesis Director

Jaime Oscar Casas Piedrafita

Instrumentation, Sensors and Interfaces Group

Universitat Politècnica de Catalunya

June 25, 2019

Abstract

Nowadays cardiovascular diseases are a main concern in the society as they impact several lives. Given the increase of lifespan humankind has experienced and the spreading of bad habit such as sedentariness, the monitorization of the cardiovascular system for all kinds of people is becoming more frequent just to detect, diagnose and treat cardiovascular problems associated to its worsening.

The main goal of this work is to study the capability to check the cardiovascular system using IPG signals in different spots of the body, allowing a brand-new versatility in the way some measures are performed. Different ECG, ICG, IPG and PPG signals will be acquired and processed to be characterized. A first study of the evolution of the pulse wave form when propagating throughout the body will be performed. The impedance IPG signals will be studied and characterized as a suitable alternative for the ICG signals, allowing both patients and medicals make measures of interest in more comfortable spots and obtain theoretically the same information.

During this thesis a device is proposed to obtain the electrocardiogram, impedance plethysmography and a photoplethysmography as well. This device is intended to be low-cost and allowing the tracking of an individual cardiovascular health using the most comfortable measures for each patient. This device has connectivity via wire along with a battery supporting over many hours of continuous operation. The visualization of these signals will be done on a computer, where a post-processing of the information could be performed as well.

Acknowledgment

As the completion of this assignment has finally ended, I would like to show my gratitude to all those who have directly and indirectly guided and helped me in writing this thesis and without who this would have never been possible.

From Oscar Casas, to whom I would like to give my deepest gratitude due his constant help. For being the one who gave me the idea and that has been there since the very beginning, for any doubt or obstacle.

To all my workmates, classmates and friends who have volunteer themselves to suffer my eternal measures and who have always been available to me, without any complain.

To all the people from Research group ISI, who have made me feel so welcomed and without who all the afternoons spent in Castelldefels would have been harder and longer.

And a final special mention to my family. For always being there and supporting me.

Contents

CHAPTER 1: CARDIOVASCULAR SYSTEM NON-INVASIVE MONITORING	1-1
1.1. Cardiovascular System monitoring need	1-1
1.2. Parameters for monitoring the cardiovascular system	1-1
1.3. Main Goal and Hypotheses.....	1-2
1.4. Proposed Solution	1-3
1.5. Current state of the art.....	1-3
1.4.1. Stroke volume from ICG	1-3
1.4.2. Stroke volume from PPG	1-4
2.4.3. Stroke volume from IPG	1-4
CHAPTER 2: THEORETICAL FOUNDATIONS	2-5
2.1. The cardiovascular system.....	2-5
2.1.1. The heart	2-5
2.1.2. The heartbeat rhythm	2-6
2.1.3. The blood vessels network	2-6
2.1.4. Stroke Volume	2-8
2.2. Biomedical Signals.....	2-8
2.2.1. Electrocardiogram (ECG)	2-8
2.2.2. Impedance Plethysmography (IPG).....	2-9
2.2.3. Photoplethysmography (PPG)	2-11
2.3. Mathematical Obtention of Stroke Volume	2-12
2.3.1. Stroke Volume from ICG	2-12
2.3.2. Stroke Volume from IPG	2-14
CHAPTER 3: SIGNAL ACQUISITIONS	3-16

3.1. Subjects.....	3-16
3.2. Devices, settings and tools	3-16
3.2.1. BIOPAC.....	3-16
3.2.2. Electrodes.....	3-17
3.2.3. Measurement Settings	3-17
3.3. Measurements Locations.....	3-18
3.2. Factors to be considered	3-19
3.2.1. Influence of Breathing	3-19
3.2.2. Influence of Filtering.....	3-21
3.2.2. Comparison between digital and analogical derivative	3-22
CHAPTER 4: SOFTWARE DEVELOPMENT	4-24
4.1. Pan-tompkins Algorithm	4-25
4.2. Characterization of IPG signals and derivative	4-27
4.2.1. Characterization of maxima and minima.....	4-28
4.2.2. Characterization of the impedance first derivative	4-30
4.2.2. Integration of the signal and the wave pulse average form.....	4-31
4.3. Computation of bioparameters of interest.	4-31
4.4. Model to be applied.....	4-32
4.4.1 Study of the sensitivity of each parameter to changes	4-33
CHAPTER 5: HARDWARE DEVELOPMENT	5-34
5.1. System Specifications.....	5-35
5.2. Required electronic elements	5-35
5.2.1. Low Pass Sallen-Key Filter.....	5-35
5.2.2. Amplifiers	5-36
5.2.4. AM Demodulation.....	5-37
5.3. Electrocardiograph	5-37

5.4. Impedance Plethysmograph	5-38
5.5. Photoplethysmograph	5-38
5.7. Power Supply	5-39
5.8. Device Usage	5-39
CHAPTER 6: RESULTS AND CONCLUSIONS	6-40
6.1. Variability of the signals	6-40
6.2. Obtention of the Stroke Volume from IPG signals	6-45
CHAPTER 7: CONCLUSIONS AND FUTURE PERSPECTIVES	7-50
Appendix A	A-51
A.1 Pan-Tompkins Algorithm	A-51
A.2 Impedance Characterization	A-55
A.3 Impedance First Derivative Characterization	A-57
Appendix B	B-65
Appendix C	C-71
C.1 ECG.....	C-71
C.1.1 ECG Schema	C-71
C.1.2 ECG Board	C-72
C.2. IPG.....	C-73
C.2.1 IPG Schema	C-73
C.2.2 ECG Board	C-73
C.3. PPG.....	C-74
C.3.1 PPG Schema	C-74
C.3.2 PPG Board.....	C-75

List of Figures

Figure 2.1. The Heart Anatomy.....	2-5
Figure 2.2. Cardiovascular System Anatomy.....	2-6
Figure 2.3. Aorta Anatomy.	2-7
Figure 2.4. Arm Arteries.	2-7
Figure 2.5: Leg Arteries.	2-8
Figure 2.6. ECG Wave Form.	2-9
Figure 2.7. IPG measure mechanism.	2-10
Figure 2.8. IPG Pulse Wave.	2-10
Figure 2.9. Impedance First Derivative Characteristic Points.....	2-11
Figure 2.10. Transmissive method on the left and reflective method on the right.	2-12
Figure 3.1. Biopac Device.	3-16
Figure 3.2. DORMO Ag/AgCl Electrodes.	3-17
Figure 3.3. EL500 Ag/AgCL Electrodes.....	3-17
Figure 3.4. Measure Positions.....	3-18
Figure 3.5. Performance of Z4 and Z7 measures in subject 4 and 2 respectively.....	3-18
Figure 3.6. Breathing In.	3-19
Figure 3.7. Recovery of the breathing rate from ECG and impedance signals.....	3-19
Figure 3.8. Erasing breathing influence using a bandpass filter.....	3-21
Figure 3.9. Band pass filtered ECG signal.	3-22
Figure 3.10. Comparison between raw and filtered ICG signal.....	3-22
Figure 3.11. Comparison between analogical and digital derivatives	3-23
Figure 3.12 Analogical and digital characterized signals.	3-23
Figure 4.1. Parameters to be found.....	4-24

Figure 4.2. Filtering the ECG signal.	4-25
Figure 4.3. Final ECG processed signal.	4-26
Figure 4.4. ECG with all peaks detected	4-27
Figure 4.5. ICG, PPG and IPG signals with minima limits.	4-28
Figure 4.6. ICG, PPG and IPG signals with maxima limits.	4-29
Figure 4.7. Characterized ICG, PPG and IPG signals.....	4-29
Figure 4.8. Impedance derivative with the E and X points limits.	4-30
Figure 4.9. Impedance first derivative with the characteristic points.	4-31
Figure 5.1. Main Schema of the hardware to be developed.....	5-34
Figure 5.2. Developed hardware.	5-35
Figure 5.3 Sallen-Key low pass filter.	5-35
Figure 5.4. A classical differential amplifier.	5-36
Figure 5.5. Classic instrumentation amplifier circuit.	5-36
Figure 5.6. Switching demodulator block circuit.	5-37
Figure 5.7. Electrocardiograph block diagram.	5-37
Figure 5.8. Impedance Plethysmograph block diagram.	5-38
Figure 5.9. Photoplethysmograph Circuit Design.	5-39
Figure 5.10. Using a weighing scale to perform IPG measures.....	5-39
Figure 6.1. Transbrachial evolution.	6-41
Figure 6.2. Transbrachial evolution with delays	6-42
Figure 6.3- Local Measures.	6-43
Figure 6.4. Local ICG signals evolution.	6-45
Figure 6.5. Dispersion Graphs	6-47
Figure 6.6. Main area defined by ejection time	6-47
Figure 6.7. Dispersion graph for each measure spot.....	6-49
Figure C.1. ECG circuit schema design.....	C-71

Figure C.2. Frontal ECG board.....C-72

Figure C.3. Rear ECG board.C-72

Figure C.4. IPG circuit schema design.....C-73

Figure C.5. Frontal IPG board.C-73

Figure C.6. Rear IPG board.C-74

Figure C.7. PPG circuit schema design.....C-74

Figure C.8. Frontal PPG board.....C-75

Figure C.9. Rear PPG board.C-75

Nomenclature

ECG: Electrocardiogram

IPG: Impedance Plethysmography

ICG: Impedance Cardiography

PPG: Photoplethysmography

SV: Stroke Volume

IA: Instrumental Amplifier

LPF: Low Pass Filter

HPF: High Pass Filter

BPF: Band Pass Filter

CARDIOVASCULAR SYSTEM NON-INVASIVE MONITORING

1.1. Cardiovascular System monitoring need

In modern societies, the need to monitor the health state of citizens and extract worthwhile information just to detect, diagnose and treat different diseases at an early stage is of utter importance. Even though recent technologies have allowed the development of a wide and diverse variety of new devices to monitor and check the cardiovascular system state, there are still a wide range of techniques and methods which are invasive and uncomfortable to perform.

According to the World Health Organization, approximately 17,9 people die each year from cardiovascular diseases, which means a 31% of all deaths worldwide [1]. Almost a 75% of all these deaths occur in low-income countries, which does not present public health services and cannot afford expensive devices to monitor the cardiovascular system of their population. Current devices to detect this state require uncomfortable methods and are quite expensive. Thus, there is an increasing need to develop new ways to check the cardiovascular state in both a cheaper and more comfortable manner.

1.2. Parameters for monitoring the cardiovascular system

Throughout this paper, the main idea is to confirm that some valuable information can be extracted from the cardiovascular system using more comfortable measures. The different approaches to a non-invasive monitoring of the cardiovascular system developed so far have been centered on the usage of the ECG signal to characterize the body electrical behavior and the use of the PPG signal to obtain the pulse wave [2]. These

both techniques will be widely explained in the subset 2.2.1 and 2.2.3 respectively. Different portable mobile devices have been developed so far aiming to facilitate the outpatient monitoring of the cardiovascular system. Some examples are wrist-worn bracelets [3] [4] and smart T-shirts [5] among others. However, these last years the IPG signals, which measure the corresponding bioimpedance of a body part and will be deeply explained in the subset 2.2.2, have been increasingly studied to obtain the pulse wave due the many advantages they present [6].

Since in 1940 was first studied and characterized [7], the IPG signal centered on the thoracic zone (ICG) has been the only one to be used and studied for years. However, it is quite uncomfortable to be measured as it requires the placement of two pair electrodes in the middle of the body side and the neck. Meaning it is not an easy measure to be performed by an individual at home without any help. Therefore, using the IPG technique in other spots would be useful to allow more comfortable measures, reporting theoretically the same information. Hence some comfortable devices such as a weighing scales or some hand device could be easily integrated with IPG measures and be used easily by old or sick people to monitor their cardiovascular system at home, without any help.

1.3. Main Goal and Hypotheses

The main aim of this thesis is to characterize the variability and keep studying further the nature and behavior of the so called IPG signals. Furthermore, the Stroke Volume will be chosen as the main objective to obtain from IPG measures, having as a final goal to develop a new way to approximate the SV value using the limbs parts of the body (hands and lower leg) and not only the thorax.

Our main hypothesis will consist on the idea that when propagating throughout the body, the pulse wave evolves differently depending on the individual. Being able to personalize, find and characterize somehow this way of propagation, IPG signals could be used to extract valuable information from the cardiovascular system.

1.4. Proposed Solution

Both a model and a device will be developed to extract an approximate value of the Stroke Volume using the information contained in these signals, once confirmed our main hypothesis and having obtained some propagation coefficient for each individual. The final goal is to demonstrate that when using an IPG method, the same information can be extracted from any spot, focusing this demonstration on the obtention of the SV value. Thus, everyone could choose the more comfortable place to monitor the cardiovascular system depending on their necessities and allowing them to perform daily or recurrent measures on their own.

1.5. Current state of the art

The cardiovascular system is a complex system that can experiment a wide and diverse range of problems and diseases. The current state of the art presents uncomfortable measure devices requiring a considerable number of electrodes and measures at a time to obtain some valuable information.

When talking about the stroke volume computation, there are different methods to obtain the stroke volume, mainly using ICG and PPG signals. The usage of different formulas may lead to quite different results. In the following part, we are going to see different approaches:

1.4.1. Stroke volume from ICG

The first approach to obtain an approximate value of the Stroke Volume was using the ICG signal as the source of information. Two main approaches have been implemented since 1940, when ICG was first started to be used to approximate the Stroke Volume and Nyöber derived a closed formula [7] that was as follows.

$$SV = \rho \frac{L_0^2}{Z_0} \Delta Z \quad (1)$$

Even though the Nyöber formula is currently still used, in 1966 Kubicek derived a second closed formula [8] that was much more accurate, which is attached below.

$$SV = \rho \frac{L_0^2}{Z_0} \frac{dZ}{dt_{max}} t_{ejec} \quad (2)$$

In both formulas, the SV is directly the stroke volume in [mL], ρ is the blood resistivity expressed in [Ω cm], L_0 the distance between both receiving electrodes [cm], Z_0 the basic impedance of the body segment limited by both receiving electrodes and the ΔZ value the variation of the bioimpedance signal, being both parameters in [Ω], $\frac{dZ}{dt_{max}}$ is the maximal amplitude of the impedance first derivative peak and t_{ejec} is the time that blood lasts to be ejected from the heart.

1.4.2. Stroke volume from PPG

Different approaches have been performed to obtain the Stroke Volume from the photoplethysmography signal of an individual. Some late studies have related the Systolic amplitude of this signal to the value of the Stroke Volume, in both fingers and ears [9]. They show there is a clear correlation between both variables.

Other investigations were pointed to approximate the value of this parameter computing the integral of the Pulse Wave and using the thoracic impedance value as a normalization factor [10].

2.4.3. Stroke volume from IPG

As most of the studies performed to approximate the value of the SV have been working with the ICG signal, there is no much bibliography regarding other IPG signals. Some studies have been done lately working with local IPG signals and trying to approximate the SV value using some equation relating the characteristic points with the SV value [11] [12]. The equation (3) is the most common used formula to compute this approximation.

$$SV = V_c \cdot \sqrt{\frac{dZ/dt_{max}}{Z_0}} \cdot t_{ejec} \quad (3)$$

Where V_c is a volume-related constant and the other parameters are the same explained in formulas (1) and (2).

THEORETICAL FOUNDATIONS

2.1. The cardiovascular system

The cardiovascular system is a vast network of organs and vessels responsible for the flood of blood, nutrients, cellular waste, hormones and some gases which go to and from cells. It consists of the heart, arteries, veins and approximately 5 liters of blood that moves continuously throughout the whole body and is made up of plasma, red blood cells, white blood cells and platelets [13].

2.1.1. The heart

The heart is a muscular pumping organ that powers the cardiovascular system. Even at rest, the average heart easily pumps over 5 liters of blood throughout the whole body every minute. It has four different chambers, two upper atria (the receiving chambers) and two lower ventricles (the discharging chambers). The atria are connected to the ventricles via the atrioventricular valves. The heart ejects blood through two different pathways:

- In the pulmonary circuit, the deoxygenated blood leaves the right ventricle via the pulmonary artery and travels to the lungs. Then it returns as oxygenated blood to the left atrium via the pulmonary vein.
- In the systemic circuit, oxygenated blood leaves the body via the left ventricle to the aorta, and from there enters the arteries and capillaries where it supplies tissues with oxygen. Deoxygenated blood returns via veins to the venae cava, reentering the heart right atrium.

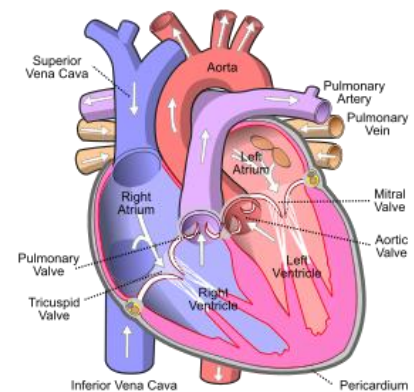


Figure 2.1. The Heart Anatomy.

The heart contains electrical pacemaker cells, which allow it to contract producing the so known heartbeats. A healthy heart contraction happens following five different steps:

1. Early Diastole: The heart is relaxed.
2. Atrial Systole: The atrium contracts to push the blood into the ventricle.
3. Ventricles start contracting without changing the volume.
4. The ventricles keep contracting while empty.
5. The ventricles stop contracting and relaxes.

Thus, blood is ejected throughout the body and the cycle repeats, to keep pumping blood.

2.1.2. The heartbeat rhythm

The pacemaker cells are the responsible to create this rhythmic impulse, setting the pace for the blood pumping, thus controlling directly the heart beat rate. The key of the rhythmic firing of the pacemaker cells is because of the slowly depolarizations this kind of cells can experiment by themselves, without needing any outside innervation. These cells constitute the Sino-atrial node which is located at the upper part of the right atrium. They can be spontaneously depolarized when a threshold potential is overcome, thanks to the change of the ionic concentration across the membrane. Once this depolarization is started, the impulse starts propagating through the conductive cells to other regions of the heart, exciting both the left and right atria and reaching the Atrio-ventricular node. Once the atria have completed its contraction, the impulse is transmitted to the ventricle, causing its own contraction. The impulse will be conducted to the apex, the lower part of the ventricles, and then propagates through the whole ventricle, originating it in the apex and propagating afterwards to the whole cavity.

2.1.3. The blood vessels network

The blood arrives to every organ and tissue thanks to a complex network of blood vessels. There are two kind of blood vessel: The arteries are responsible to take the blood ejected from the heart to the whole body and the veins transport the blood back to the heart. To arrive to every spot of the human body, vessels ramify in tinier ones, going from centimeters of diameter like the Aorta to almost millimeters like the vessels of the hands.

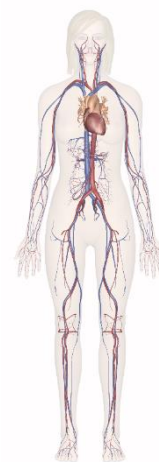


Figure 2.2. Cardiovascular System Anatomy.

The most important contribution to the IPG signal is the corresponding arterial change of volume [14]. Due their work mechanisms, veins do not change their volume as much as arteries, because they tend to remain rigid. Therefore, it is important to characterize the arterial system present in both thorax and limbs to understand some effects that can be observed in the IPG signals.

2.1.3.2. Aorta

Aorta is the largest artery of the human body. Beginning at the top of the left ventricle, the heart pumps blood from the left ventricle to the aorta through the aortic valve. Three different leaflets on the aortic valve open and close with each heartbeat to allow just a one-way flow of blood. It is a huge tube of about half a meter and three centimeters of diameter. It is divided in four distinct parts:

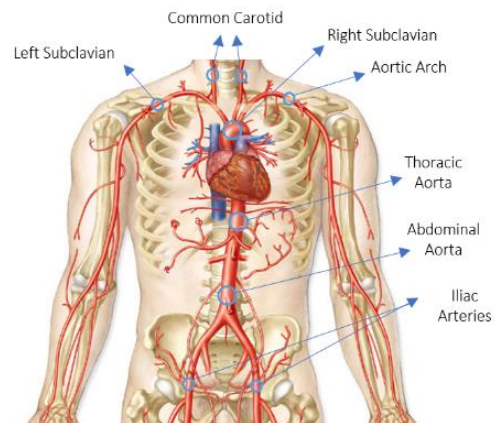


Figure 2.3. Aorta Anatomy.

1. The aorta starts rising from the heart.
2. Then comes the Aortic Arch, which curves over the heart and presents some little vessels that supply blood to the head and to the left and right arm being called Common Carotid and the Left and Right Subclavian respectively.
3. Then it starts descending forming the thoracic aorta, travelling through the chest and bringing blood to ribs and some chest structures.
4. The final abdominal aorta starts at the diaphragm and splits in two paired iliac arteries in the lower abdomen.

2.1.3.2. Arm Vessels

Blood begins the journey into the arm by leaving the aortic arch and entering one of the two subclavian arteries. When entering the arm, the Brachial artery begins being the major artery of the upper arm. Then it travels down the elbow until it splits into the Radial and the Ulnar arteries.

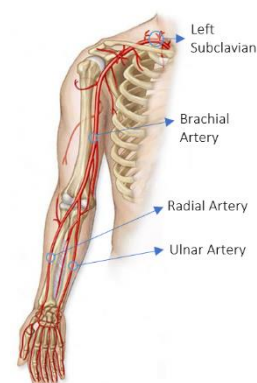


Figure 2.4. Arm Arteries.

2.1.3.3. Leg Vessels

Just below the kidneys, the abdominal aorta splits in two main branches known as the common iliac arteries. Each of them travels down one leg, splitting just after the knee into peroneal and tibial arteries.

2.1.4. Stroke Volume

The stroke volume is the volume of blood pumped from the left ventricle each heartbeat. It is commonly ranged between the 40 and 100 mL, depending its value on a wide variety of factors such as age, mass-weight, health condition and genre among others. It

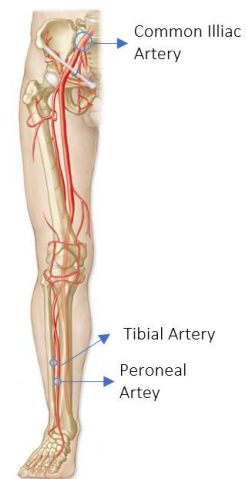


Figure 2.5: Leg Arteries.

is one of the main parameters to characterize and check the good state of the cardiovascular system. As it decreases in certain conditions or changes due some diseases such as cardiogenic shock, hemorrhage and sepsis among others, stroke volume can be easily correlated with the cardiac function [15]. Despite its clinical significance, so far Stroke Volume has not been commonly used for routine diagnostic and monitoring purposes due its difficulty to be measured.

2.2. Biomedical Signals

2.2.1. Electrocardiogram (ECG)

The electrocardiogram is the signal that accounts for the electrical activity of the heart. The measure is based on the recording of the voltage versus time of such electrical activity using electrodes placed on the skin, giving as an output a quasi-periodical rhythmically repeating signal. It measures the existing potential between two points of the body surface, containing the information about the projection of the polarization vector of the heart.

Some characterization points can be easily related to some bio parameters. The ECG signal consist in different waves called as the consecutive letters P, Q, R, S and T. Each wave corresponds to a different stage of the depolarization of the heart, having all of them information of the corresponding part of the process [16].

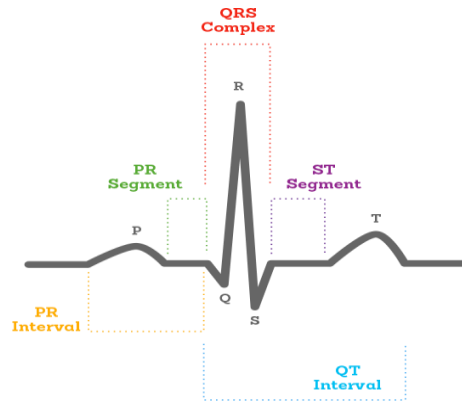


Figure 2.6. ECG Wave Form.

The origins of each of these waves are explained as follows:

- The P wave represents the beginning of the heartbeat, being it the atrial depolarization. The contraction of the atrium takes place during this stage.
- The QRS complex represents the ventricular polarization. As the ventricle contracts, the blood is ejected from the heart.
- The T wave represents the ventricular repolarization, when the ventricles relax and distends.

The main characterization point of the ECG signal is the position of the QRS peak, which indicates the ejection of the blood from the left ventricle. It is widely used to obtain certain parameters such as the Heartbeat Rhythm.

2.2.2. Impedance Plethysmography (IPG)

Electrical Impedance Plethysmography is a non-invasive method based in electrical impedance phenomena for measuring the pulse wave propagation throughout the body. It is based on the idea that the blood flowing has a much lower impedance than the surrounding tissue, thus making that impedance decreases when blood arrives. The body electrical impedance can be divided in a basal component (Z_0), which remains constant and is produced by the tissue, fats and bones and a variable one (Z), which accounts for the changes on volume due blood arrival. Therefore, the IPG signal variation depends directly on a change in the volume of arteries produced due the pulse wave propagation.

Four electrodes are connected to the body part of interest to measure. A low frequency and alternating current of very small amplitude is applied to the body. The resulting signal

can be characterized to obtain information such as the breath modulation, the state of the arteries or some bioparameters of interest. The electrical current is applied on the two outer electrodes and the corresponding variation in the voltage is measured in the inner electrodes.

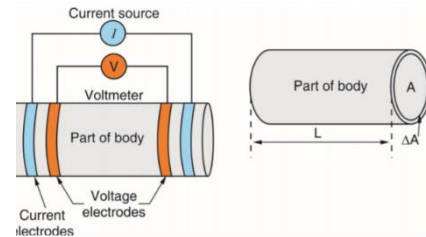


Figure 2.7. IPG measure mechanism.

It is important to consider that the IPG signals are usually inverted, as the understanding of the inverse function is much more intuitive. Hence when blood arrives the impedance decreases, but in the graph an increasing curve can be observed. Each cardiac cycle appears as a peak, presenting some distinct stages [17] [18], which can be observed in the following figure 2.8.

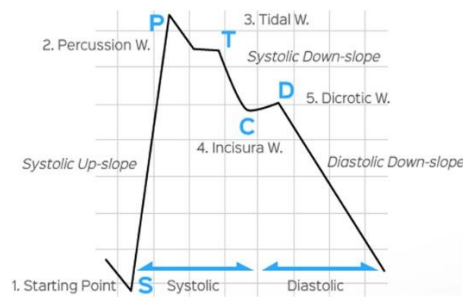


Figure 2.8. IPG Pulse Wave

The general IPG wave can be characterized as follows:

- **Starting Point (S):** The first flat region before the blood has arrived.
- **Percussion Wave (P):** Taking place during the systole, it is caused mainly by the cardiac ejection when the blood is ejected from the left ventricle.
- **Tidal Wave (T):** Although it is not always visible, it is the result of the reflection of the percussion wave in the arterial branches.
- **Dicrotic Notch (C):** Flat region that indicates when the closure of the aortic valve takes place.
- **Dicrotic Wave (D):** The closure of the aortic valve produces an elastic recoil on the arterial vessels which generates a second increase of the pressure.

In the case of the IPG signal, not only the signal itself contains information, but its first derivative. The characterization of the first derivative can be used to obtain worth information such as the stroke volume, as it will be later explained in the subset 2.3. In the figure 2.9, one can observe the different points of interest and their meaning [18].

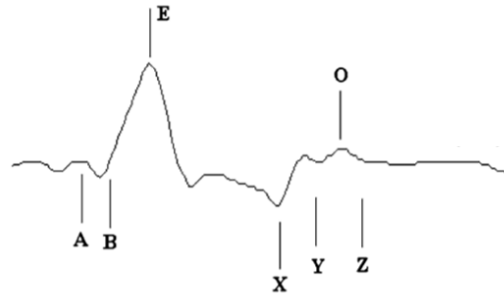


Figure 2.9. Impedance First Derivative Characteristic Points.

- A. This wave is associated with the atrial contraction and its amplitude is correlated with the ejection fraction of the left atrium.
- B. This wave is associated with the opening of the aortic valve. It occurs on the ascending part of the ICG curve, before the first derivative takes its maximum value. Denotes the beginning of the ejection time.
- E. This point is placed on the top position of the curve reflecting the maximal speed of the change in the impedance.
- X. Corresponds to the closure of the aortic valve. Described as a minimal value of the first derivative, occurring after maximum E point.
- Y. Corresponds to the closure of pulmonic valve.
- O. This wave is associated with changing of the volume during the diastolic phase of the cycle and opening snap of the mitral valve.
- Z. This wave describes a decreasing following the O wave.

During the work, the most used characteristics points will be the B, E and X points of the first derivative of the impedance signal, as they are the most commonly used points in the bibliography to approximate the SV value [11].

2.2.2.1. Impedance Cardiography (ICG)

Impedance Cardiography, also called as transthoracic electrical impedance plethysmography was first named in 1940. It consists in the same IPG method but performed in the transthoracic part of the body [18]. ICG is a non-invasive method for finding the change of transthoracic total electrical impedance with the change of blood volume in the transthoracic region. It is the most commonly used and widely studied plethysmography technique, thus having an own name and being differentiated from the rest of the IPG signals.

2.2.2.3. Photoplethysmography (PPG)

Photoplethysmography is a simple and low-cost optical technique that can be used to detect cardiac-induced blood volume changes in the microvascular bed of tissue. The

change in volume that the pressure wave causes is detected by illuminating the region of skin with the light from a LED (light-emitting-diode) and then measuring the amount of light either transmitted (Transmissive method) or reflected (Reflective method) to a photodiode.

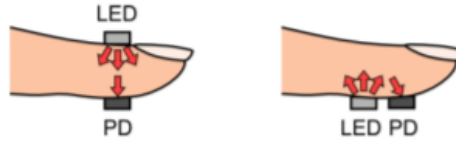


Figure 2.10. Transmissive method on the left and reflective method on the right.

Each cardiac cycle appears as a peak. The corresponding PPG waveform consists of two peaks, one from the first ejection of blood (direct wave) and a second one coming from the reflected wave [19].

2.3. Mathematical Obtention of Stroke Volume

2.3.1. Stroke Volume from ICG

As it has already explained in the *Chapter 1*, there are two main models to obtain the SV from ICG: The Nyboer and the Kubiceck models. To obtain both models, some approximations were made. In a very simple way, the impedance of the thorax can be described as two different impedance: the one coming from the tissue and bones and the one generated by fluids [17]. As the amount of blood in the thorax changes with the heart cycle, during systole, the left ventricle ejects an amount of blood equal to the stroke volume wanted to be measured. The change of this amount of blood can be easily measured when registering the changes of impedance in the thorax.

Considering both impedances present in the thorax, Z_b (*blood impedance*) and Z_t (*tissue impedance*), the total impedance can be measure as in parallel:

$$Z = \frac{Z_b Z_t}{Z_b + Z_t} \quad (4)$$

The relation between the impedance change of the thorax and the impedance change of blood volume is found by differentiating the equation with respect Z_b .

$$dZ = \frac{Z^2}{Z_b} dZ_b \quad (5)$$

Assuming now a cylindrical geometry, one can say that the equivalent impedance of the blood should follow:

$$Z_b \sim \frac{\rho_b l}{A_b} \quad (6)$$

Being ρ_b the blood resistivity, A_b the cross-section of the blood Area and l the length of the thorax model. Now, as the changes in volume are to be obtained, first the last equation is multiplied by a factor l .

$$l \cdot Z_b \sim \frac{\rho_b l^2}{A_b} \rightarrow l A_b \sim \frac{\rho_b l}{Z_b} \rightarrow V_b \sim \frac{\rho_b l}{Z_b} \quad (7)$$

Now the differentiation of the equation to obtain the increment of volume is done.

$$dV_b \sim -\rho_b \frac{l^2}{Z_b^2} dZ_b \quad (8)$$

2.4.1.1 Nyboer Formula

Atzler and Lehman suggested for the first time that changes in electrical impedance of chest could be related to the blood volume going across the thorax during one cardiac cycle. However, it was not until Nyboer investigations who derived a closed formula to obtain an approximate value of the stroke volume, which can be directly obtained from the mathematical development made before and the first published paper [7].

Substituting $dV_b = \Delta V \sim SV$ and $dZ_b \sim \Delta Z$ the SV value is obtained as

$$SV = \rho \frac{L_0^2}{Z_0^2} \Delta Z \quad (1)$$

2.4.1.2. Kubicek Formula

After Nyboer publication, Kubicek was the one to modify his formula replacing the impedance increment by two new parameters, which was supposed to be more accurate and can be found in the following paper [8]. In the process, Kubicek made some assumptions. As it was mentioned earlier, during systole the right ventricle ejects a given amount of blood into the lungs, thus obtaining its value from the increment of impedance

it produces. However, if it is assumed that no blood was to flow away from the thorax during systole, the thorax impedance would continuously decrease during systole at a rate equal to the maximum derivative value of decrease of Z during the ejection time. Therefore, the increment of impedance can be approximated using the ejection time and the maximum derivative of the impedance.

$$SV = \rho \frac{L_0^2}{Z_0} \frac{dZ}{dt}_{max} t_{ejec} \quad (2)$$

The Kubiceck formula has been the most widely used, giving much more accurate values of the Stroke Volume. Multiple devices and systems have been developed to approximate accurately the SV, not being so far used in clinical methodologies.

2.3.2. Stroke Volume from IPG

To derive the required equation to relate the IPG signals with Stroke Volume, one must first consider some main ideas. First, impedance is not a time directly dependent variable. The impedance of a body part changes following both the changes of volume that the arteries suffer due the blood arrival and the changes of the velocity of blood. Thus, the Z value is varying in function of the velocity and volume of blood for a given instant, but not with the time itself. However, during this thesis, the approximation that the impedance changes with time will be used, considering that both velocity and volume of blood do change with time.

$$\Delta Z(f(v, V)) \sim \Delta Z(t) \quad (9)$$

Now the cylindrical assumption derived in equation 7 is used. Differentiating this last equation, one obtains:

$$\frac{dZ}{dt} \sim \frac{L^2}{V_b} \frac{d\rho_{b(t)}}{dt} - \frac{\rho_b L^2}{V_b^2} \frac{dV_b}{dt} \quad (10)$$

$$(A) \quad (B)$$

(A) and (B) represent respectively the ohmic mean acceleration and the ohmic mean flow velocity. However, it has been found that dZ/dt_{max} must be a blood acceleration and not a velocity or flow [20]. Therefore, the second term is negligible, and the final relation is obtained.

$$\frac{dZ}{dt} \sim \frac{L^2}{V_b} \frac{d\rho_b(t)}{dt} [\Omega \cdot s^{-2}] \quad (11)$$

To reduce an ohmic mean acceleration to ohmic mean velocity, a normalization and a square root are applied in the equation (11) obtained formula to make the dimensionality be coherent.

$$v_{ohmic} = \sqrt{\frac{dZ(t)/dt_{max}}{Z_0}} = \sqrt{\frac{L^2}{V_b} \frac{\rho_b(t)}{dt} \frac{1}{Z_0}} [s^{-1}] \quad (12)$$

To finally obtain the Stroke Volume, this ohmic mean acceleration is multiplied by the ejection time, which in this case is the time while blood is arriving in the measured zone, and a volumetric thoracic-related constant.

$$SV \sim V_c v_{ohmic} t_{ejec} = V_c \sqrt{\frac{dZ(t)/dt_{max}}{Z_0}} t_{ejec} \quad (3)$$

The volumetric constant V_c , otherwise known as the volume of electrically participating tissue presents a high linear relationship and high correlations with the corporal weight [21] and is usually approximated by the following relation.

$$V_c \sim 32 \cdot W^{1.02} \quad (13)$$

SIGNAL ACQUISITIONS

3.1. Subjects

A total set of 15 people were measured and recorded in the development of this thesis. From them, 11 were used to perform the approximation of the Stroke Volume value from different IPG signals.

Males / Females	4 (37 %) / 7(63%)
Age	22 ± 4 years
Weight	70 ± 15 kg

Table 1. Characteristics of the total set of subjects.

3.2. Devices, settings and tools

3.2.1. BIOPAC

The device used to record all required signals to perform the characterizations during the first stage of the thesis was a BIOPAC MP36R, which is a four-channel data acquisition system with 24 bits of resolution for life science research. The device presents an internal microprocessor that allows to control data acquisition and communication with the computer. Regarding the safety, the device presents both Medical Safety Test Standards (IEC 60601-1) and the Medical Electromagnetic Compatibility (60601-1-2).



Figure 3.1. Biopac Device.

When talking about the specifications, it presents both software and hardware filters that can be used. In our case, just the both low and high hardware filters were used, which

will be explained in the subset 3.2.3. It works in DC with the frequencies of 0.05, 0.5 and 5 Hz. It presents a wide range of gains as well, from 5x to 50,000x [22].

3.2.2. Electrodes

Electrodes are relatively simple transducer elements that attach to the surface of the skin and pick up electrical signals of the body. Two different kind of electrodes were used during the measures performed in the thesis.

For the IPG signal, the EL500 electrodes of BIOPAC systems were used. They are Ag/AgCl dual electrodes with high adhesion and high conductivity. The two contacts of the electrodes present a fixed spacing. They incorporate a gel cavity situated between the electrode and the skin surfaces, which allows to reduce motion artifact.

For the ECG signals, the SF-36 ECG electrode of DORMO was used. It presents a dry gel that improves the conductivity and consists of common Ag/AgCl electrodes with high adhesion.

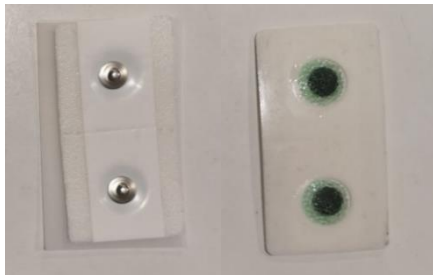


Figure 3.3. EL500 Ag/AgCL Electrodes.



Figure 3.2. DORMO Ag/AgCL Electrodes.

3.2.3. Measurement Settings

The different signal measurements were performed using the following Biopac device settings.

Signal	Biopac Settings
Z_0	Low Pass Filter with $f_l = 0.5$ Hz and $G = 1000$.
IPG/ICG	High Pass Filter with $f_h = 0.5$ Hz. and $G = 1000$.
IPG/ICG derivative	No filter and $G = 200$
ECG	Band Pass Filter of 0.05-100 Hz and $G = 1000$
PPG	High Pass Filter with $f_h = 0.5$ Hz. $G = 5000$.

Table 2. Biopac settings to perform the measurements.

3.3. Measurements Locations

The main idea was to choose and repeat a set of IPG measures for each subject for its subsequent characterization. Therefore, eight different IPG measures were performed simultaneously with the reference signals of ECG and PPG (in the finger). Some of them were repeated both while breathing and holding breath. The sampling frequency used was of 2000 Hz.

Z1 *ICG:* ICG signal is recorded setting two electrodes in the Neck and two more in the thoracic side.

Z2 *Measure from neck to wrist:* Two electrodes are placed in the neck and the other two in the wrist.

Z3 *Measure from the upper arm to wrist:* Two electrodes are placed in the upper arm and two more in the wrist

Z4 *Measure from the upper forearm to wrist:* Two electrodes are placed in the upper forearm and two more in the wrist.

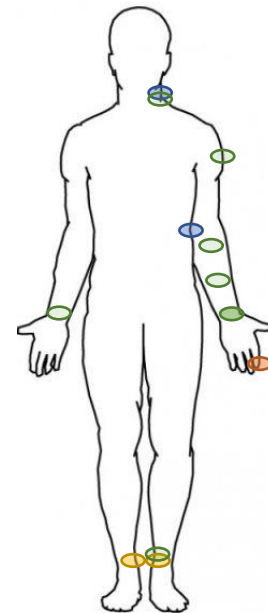
Z5 *Measure from the lower forearm to wrist:* Two electrodes are placed in the down forearm and two more in the wrist.

Z6 *PPG in the index left finger.* PPG will be acquired as a reference signal and to make some punctual comparisons.

Z7 *Measure from arm to arm:* Two electrodes are placed in the left wrist and two more in the right one.

Z8 *Measure from leg to leg:* Two electrodes are placed in the left lower leg and two more in the right lower leg.

Z9 *Measure from wrist to leg:* Two electrodes are placed in the wrist and two more in the left lower leg.



- Fixed electrodes for Leg to Leg
- Fixed electrodes for ICG
- Wrist fixed pair of electrodes
- Moving pair of electrodes
- PPG sensor.

Figure 3.4. Measure Positions.

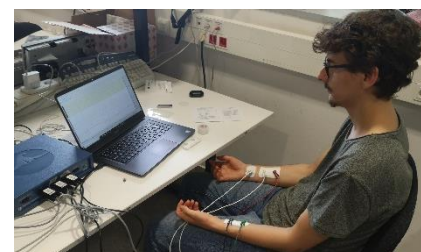


Figure 3.5. Performance of Z4 and Z7 measures in subject 4 and 2 respectively.

3.2. Factors to be considered

3.2.1. Influence of Breathing

Breathing modulates the impedance signal causing its fluctuation around the basal impedance Z_0 and results in a moving of the first derivative signal as well. As it can be seen in the figure 3.5, it is obvious that the breathing introduces in the impedance signal a moving corresponding to the breathing cycle.

Throughout this paragraph, the variability of the breathing influence will be studied, just to know if the

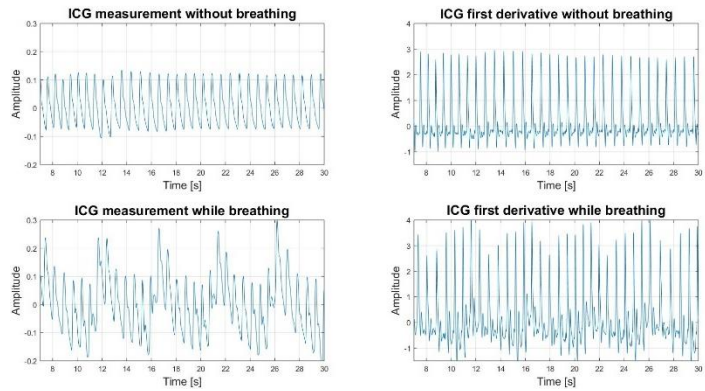


Figure 3.6. Comparison between measuring while breathing or holding the breath.

parameters of interest that are to be found will be affected by this new factor. Moreover, some filters will be applied to see if the effect of breathing can be eliminated when knowing the breathing frequency.

To begin, the first question to be solved will be if it is possible to obtain only the respiratory rate. To do so, respiratory rate of 0.2 Hz was forced. The main objective was to process the output impedance and ECG signals to recover the respiratory rate one would expect, being it an approximate sinus of 0.2 Hz of frequency. To the signals attached in the figure 3.6 a bandpass filter from 0.15 to 0.25 Hz was applied, obtaining as the result the original respiratory rate.

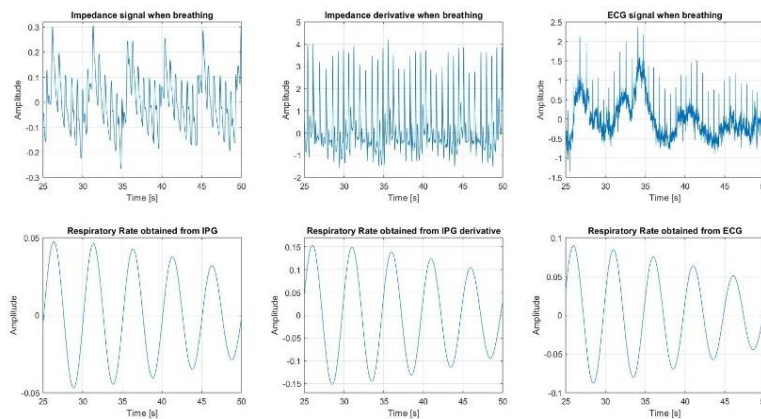


Figure 3.7. Recovery of the breathing rate from ECG and impedance signals.

It is interesting to observe that from any of the three signals (impedance, impedance derivative or ECG) one can recover the respiratory rate. Once we know how to obtain the influence of the respiratory rate, the next natural question is to avoid its influence in the signals. To do so, there are two different methods [18].

3.2.1.1. Temporary Elimination of Breathing

In this first case, the subjects were asked to hold the breath, obtaining a smoother signal with less noise. The same procedure was performed with five different subjects, just to compute the variability the breathing influence added on the signals. To show this variability, the standard deviation for each variable of interest is computed in the ICG signals measured both allowing and not allowing breathing. The results of three of these subjects are shown in the table 3. As it can be seen, when the subjects breath the standard deviation increases, adding noise to the signals.

	Subject 1		Subject 3		Subject 4	
	Holding Breath	Breathing	Holding Breath	Breathing	Holding Breath	Breathing
IPG Maxima	0.109	0.115	0.039	0.047	0.056	0.062
IPG Minima	0.086	0.088	0.097	0.101	0.027	0.045
B Point	0.076	0.087	0.019	0.027	0.045	0.056
E Point	0.078	0.087	0.010	0.021	0.047	0.055
X Point	0.082	0.086	0.09	0.023	0.044	0.056

Table 3. Standard Deviation of the obtention of the characteristic points from breathing and holding breathing measures.

3.2.1.2. Digital Filtering

In this second case, a high-pass filter was applied with a cutoff frequency higher than 0.5 Hz, in this case erasing the influence of breathing as the breathing rate usually stands under the 0.5 Hz.

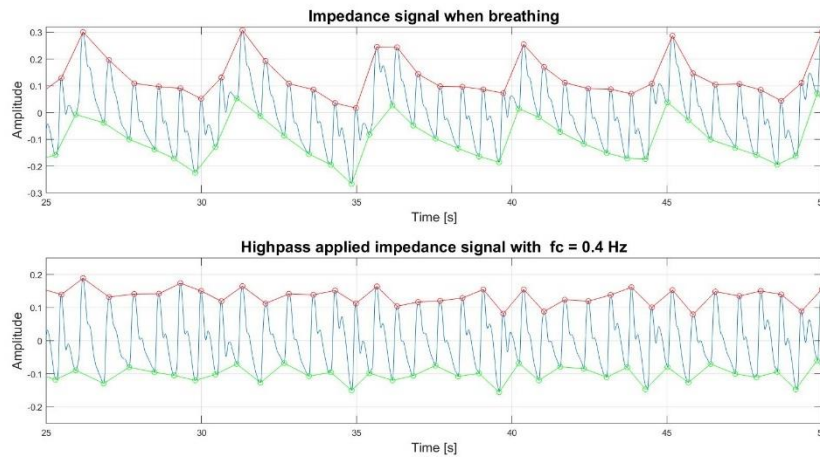


Figure 3.8. Erasing breathing influence using a bandpass filter.

As it can be observed in the figure 3.8, the resulting signal is much smoother and less noisy. In this case, holding breath is a much more effective way to decrease the noise coming from the breathing, as it is easier than force the subjects to breath with a certain frequency.

3.2.1.3. Comparison between breathing and holding breath

Knowing that recording a measure while breathing adds noise, a comparison between the results obtained from signals measured when breathing and holding breath was necessary to see how these values change. The breathing adds some variability to the signal, and as it is not controlled, it cannot be easily erased with some filter. However, as it can be seen in the table 4, the difference of both values when breathing and holding breath is not so big. It is important to notice that the main goal is not to obtain a precise number, but a guiding value.

Subject	SV while breathing	SV while holding breath	Difference (%)
S1	69.28	63.46	-8.40%
S3	43.89	40.02	-8,82%
S4	54.45	57.88	6.30%
S12	70.82	65.73	-7,16%

Table 4. Comparison between the stroke volume value obtained while breathing and while holding the breath.

3.2.2. Influence of Filtering

To obtain smoother signals, some filters can be applied to reduce the noise. One of the main problems that impedance and biomedical-related signals present is the high contribution of unwanted interferences. To do so, after a bibliographic study, two frequency ranges were found for both ECG and IPG.

To start, ECG signals present a frequency range that goes from 0.05 Hz to 100 Hz. However, the main valuable information is contained between the 0.1 and the 20 Hz [23] [24]. As the ECG signals usually contains a big noisy contribution such as the power-line interferences (between 50-60 Hz), muscle contraction noises and low-frequency components (< 1 Hz), a band-pass filter can be applied from the 0.5 to 40 Hz just to erase all the unwanted noise and conserve the most essential information, that in our case is the position of the QRS peaks. In the figure 3.9, one can easily observe how the filter does not move the position of the peaks, thus not losing any information and erasing any noise that could interfere it.

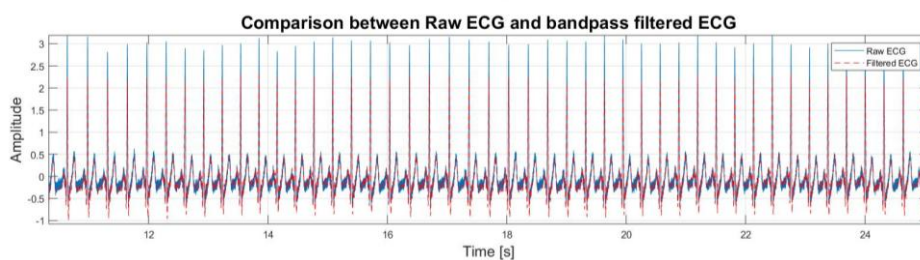


Figure 3.9. Band pass filtered ECG signal.

When working with impedance signals, the frequency range goes from 0.1 to 20 Hz [18]. As the IPG signals contain as well noisy interferences, a band-pass filter from 0.5 to 20 Hz to erase all the unwanted noise. It is important to notice not much information is lost with the application of this filter, as it can be seen in the following attached graph.

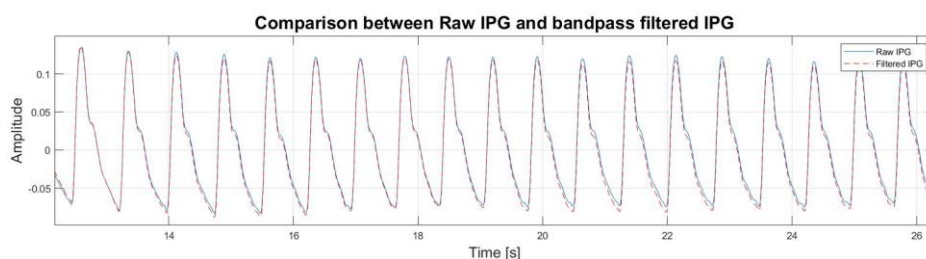


Figure 3.10. Comparison between raw and filtered ICG signal.

3.2.2. Comparison between digital and analogical derivative

Using the Biopac MP36 device, the first impedance derivative was analogically obtained when measuring the impedance signal. However, as one of the goals of the project was to develop a hardware device able to obtain some signals of interest (ECG, IPG, ICG, PPG and Z_0), the idea to obtain the derivative in a digital way was of utter interest, as it is

required to find some characteristic points. The obtention of the digital impedance derivative was performed with the following steps:

1. Band Pass Filter between 0.5 – 40 Hz.
2. Computation of a numerical derivative.

A first comparison between both signals is performed to see if they maintain the same behavior and how different both derivatives are. The comparison was performed for an ICG, upper forearm-wrist (Z4) IPG and an arm to arm (Z7) IPG signals. As it can be seen in the figure 3.11, one can observe both digital and analogical derivative present the same behavior and are quite similar.

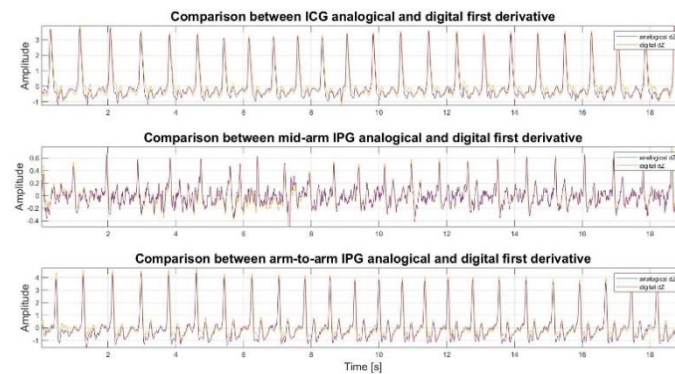


Figure 3.11. Comparison between analogical and digital derivatives

Once the comparison between the both ways to obtain the first derivative are compared, the characterization of both signals is performed. As the main goal of the first derivative of the impedance is to obtain the B, E and X characteristic points, a comparison between the obtention of these three points is required. It is interesting to observe, that while for the analogical signal the B point always coincide with a zero value, for the analogical derivative this does not always happen, losing some accuracy.

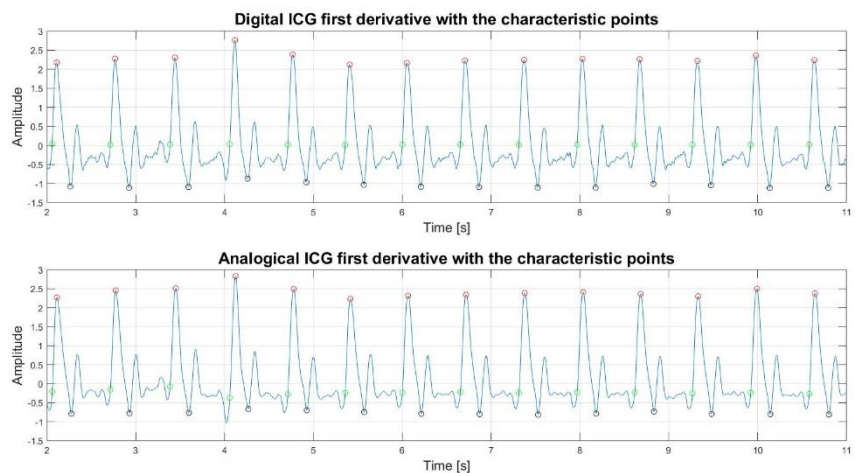


Figure 3.12 Comparison between the B points obtained from a digital and an analogical derivative.

SOFTWARE DEVELOPMENT

The first steps were to see how the pulse wave evolved when blood is ejected from the heart and started to circulate across the body. To do so, the different signals were measured and characterized to obtain some parameters of interest.

Time between QRS peak and minima of a wave pulse: Time that the blood lasts from getting ejected from the heart and to arrive to the spot where the measure takes place. Mathematically it is found from the difference between the minimum of a pulse wave and the QRS peak from the ECG. It should be bigger as further the spot from the heart is.

Time between QRS peak and maxima of a wave pulse: The time between the moment the blood is ejected from the heart and the moment when all the blood has arrived and is already leaving from the spot where the measure takes place. It should be bigger as further from the heart the spot is.

Slope of the IPG between the minima and the maxima: The slope of the first increase of the pulse wave can be related to the amount of blood that arrives to the spot. The main hypothesis is that the bigger the amount of blood is, the bigger slope of the signal must be.

Integration of the signal: The amount of blood is wanted to be related as well with the integration of the signal. The bigger the amount of blood is, the bigger the integration should be.

In addition, some characteristic points in the ECG, IPG and IPG first derivative will be found as well.

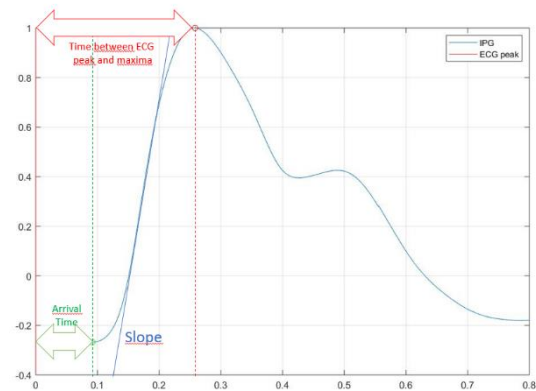


Figure 4.1. Parameters to be found.

- ECG peak indexes.
- IPG and PPG maxima and minima.
- IPG first derivative B, E and X characteristic points.

To obtain all these parameters of interest, a specific software will be developed in Matlab to characterize each measured signal.

4.1. Pan-tompkins Algorithm

The Pan-Tompkins algorithm has the main function to detect the QRS peaks of an ECG signal and was first developed by Jiapu Pan and Willis J. Tompkins in 1985 [25], becoming one of the most worldwide used algorithm to detect the QRS peak of ECG signal. The development of this algorithm was the first step in the software development, wanting to develop an algorithm that was both functional and fulfilling our necessities. The Pan-Tompkins algorithm can be found in the appendix A.1. The code can be divided in two main steps:

Step 1: Preparation of the signal

In this first part of the code, the ECG signal is processed using different filters and function to erase the noise and make the peaks more visible and distinguishable. The steps consist on:

Filtering

The first step consists on applying filters that reduce the presence of unworthy noise and makes easier to detect the main QRS peaks. Knowing that the maximum energy of the QRS peaks are found between the 5 and 15 Hz frequency range, a first band pass filter with a range of 5 and 12 Hz high, thus obtaining a new signal where the peaks are easier to be detected. The same result can be obtained applying first a high pass filter and then a low pass filter.

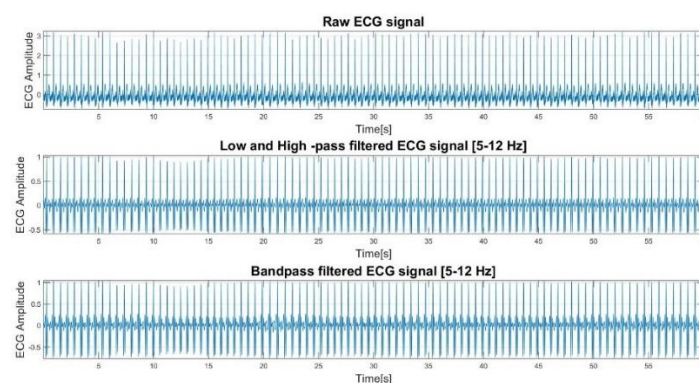


Figure 4.2. Filtering of the ECG signal.

Derivative:

Once the signal has been filtered, it is differentiated to provide the QRS slope information. The difference equation used in our case will be:

$$y(nT) = \frac{1}{8T} [-x(nT - 2T) - 2x(nT - T) + 2x(nT + T) + x(nT + 2T)]$$

Squaring Function

After the signal has been differentiated, it is squared point by point to amplify nonlinearly its magnitude emphasizing the higher frequencies and making all points positive. The equation will be as follows:

$$y(nT) = [x(nT)]^2$$

Moving Window Integration

The fourth step will be applying a moving window to convolute both signals. This integration is applied due the multiplicity of peaks during a single QRS peak. Thus, applying a moving window, all peaks near a QRS peak disappear obtaining just some visible bigger peaks that will be close to the ones corresponding to actual QRS peaks. In this case, the equation applied will be as follows:

$$y(nT) = \frac{1}{N} [x(nT - (N - 1)T) - 2x(nT - (N - 2)T) + \dots + x(nT)]$$

The wide length of the moving window is defined to not to mix different QRS peaks. In our case the length was of the 20% of the sampling frequency. As it can be seen in this last figure, the final obtained signal just presents main peaks in close position to the ones a QRS complex should be found.

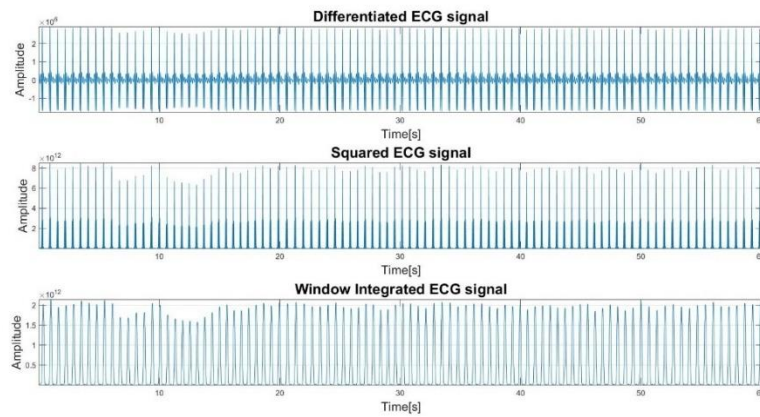


Figure 4.3. Final ECG processed signal where only the peaks are observed.

Step 2: Thresholding and location of the peaks

In this second part of the algorithm, the main idea is to select the correct peaks of the raw-ECG signal corresponding to real QRS complexes.

Peaks of Window Integrated Signal: First all the peaks of the window integrated signal are found, as they present similar position to the QRS peaks in the raw ECG signal.

Thresholding: Once we have the spots of the windows integrated signal peaks, evolving with time thresholds are computed and stored just to differentiate between real QRS peaks in the raw ECG signal and false QRS peaks. To do so, for each peak in the windows integrated signal, maxima near its spot are found in the raw ECG signal and decided to be actual QRS peaks or not.

Verification: To obtain real QRS complexes and not to commit errors, some verifications are performed during the location of peaks. Once some peaks are located, the mean distance between them is computed to assure that all peaks located maintain the same approximate distance between them. Thus, assuring no peak is left behind or added.

T-Wave Detection: As T-Wave present peaks as well, a condition with slopes is imposed to differentiate between QRS peaks and T-Wave peaks.

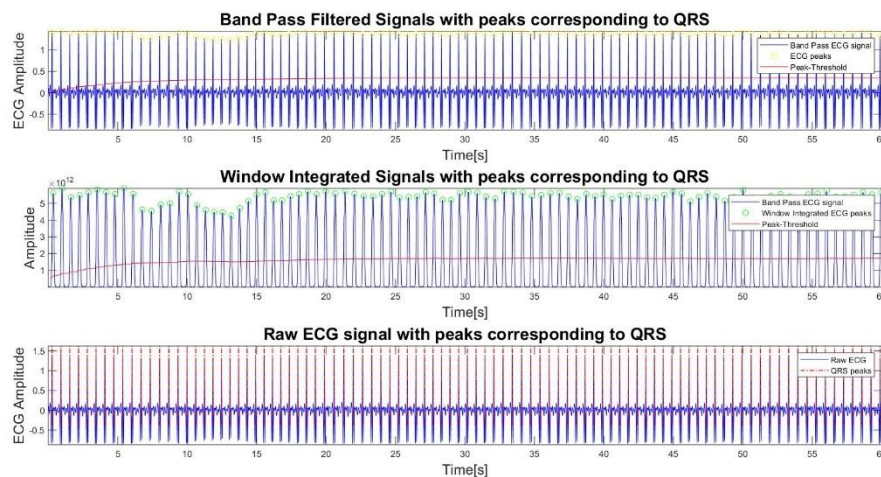


Figure 4.4. Bandpass filtered and windows integrated ECG signals with the thresholds. A last ECG signal with all peaks detected.

4.2. Characterization of IPG signals and derivative

Once obtained the Pan-Tompkins algorithm, a second algorithm was required to characterize the IPG signals and its derivative. As the main goal of the work was to extract some worth information from ICG and IPG signals, an algorithm able to extract the

wanted information and that could fulfill our necessities was required. To start, a first algorithm was designed to obtain the maxima and minima of ICG, IPG and PPG signals. It is important to notice that all IPG, ICG and PPG characterization software will require as a pattern signal the corresponding ECG at the same time.

4.2.1. Characterization of maxima and minima

To start developing the algorithm to find maxima and minima of our signals of interest, a first research about the signals that were to be characterized was done. Knowing that both minima and maxima of the signals were located just after the ECG QRS peaks, the algorithm was developed using this characteristic. The final algorithm is attached in the appendix A.2. Therefore, this first algorithm consists of two distinct parts.

ECG characterization: The associated ECG of the signal to be processed is characterized using our Pan-Tompkins function, just to obtain the locations of the ECG QRS peaks.

Maxima and Minima finding: Depending on the type of signal that is introduced, a down limit and an upper limit are defined, based on the location of the QRS signal and both the maximum and the minimum inside these limits are the local maximum and minimum of the signal.

When looking for minima, the ICG, PPG and Neck IPG signal will present their minima between the ECG peak location (red lines) and the ECG peak location plus the eighth part of the mean distance between ECG peaks (black line). When talking about IPG signals in other spots, as the minima is displaced to the right as the place of measurement gets further of the heart, the limits are set between the ECG peak location plus the eighth part of the mean distance between peaks (yellow line) and the ECG peak location plus the fourth part of the same distance (black line).

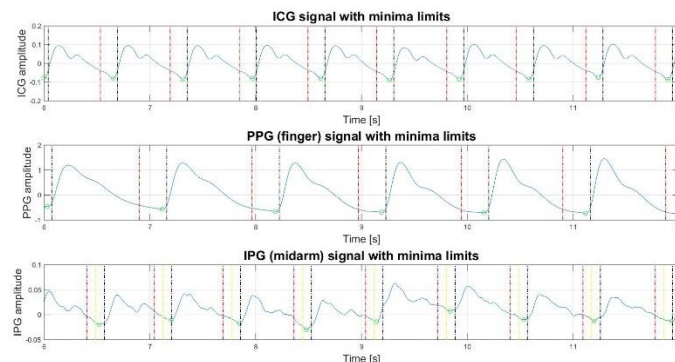


Figure 4.5. Three different ICG; PPG and IPG signals with the limits to find the maxima. Signals acquired from different subjects and in different moments.

When looking for the maxima, all signals are set the same limits. The bottom limit will be the ECG peaks and the upper limit will be the ECG peak location plus $0.45 \cdot f_s$.

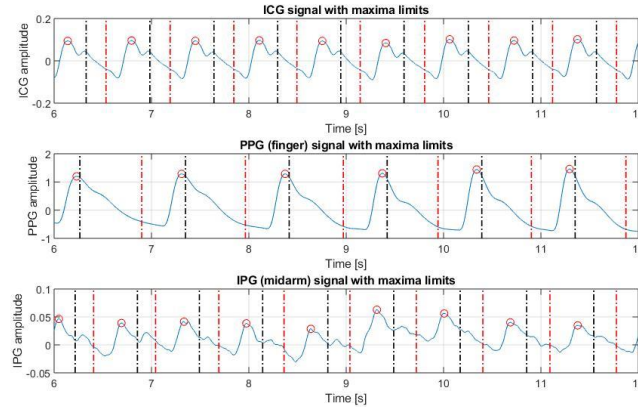


Figure 4.6. Three different ICG; PPG and IPG signals with the limits to find the maxima. Signals acquired from different subjects and in different moments.

Finally, the maxima and minima of the signals of interest can be found as shown in the figure 4.7.

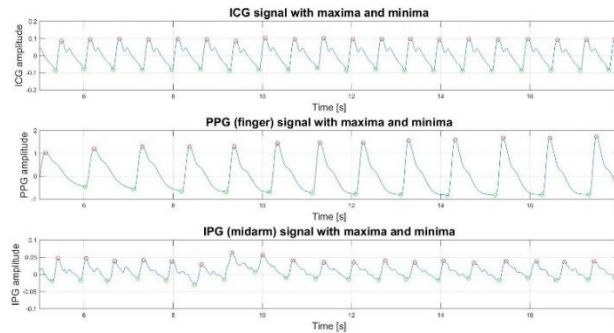


Figure 4.7. Three different ICG, PPG and IPG signals with the corresponding maxima and minima. Signals acquired from different subjects and in different moments.

It is important to notice that there can be errors in the detection of the exact position of both maxima and minima of signals. When acquiring a signal, a sampling frequency is used which in our case was of 2000 Hz. At first, there is a limited accuracy of $1/f_s$. In case of maxima, this accuracy limit is quite correct, as peaks are really pronounced and cannot be confused with other big values. Hence the limits set to find the maxima are wider than for minima, as they cannot be confused.

However, when locating minima, as there is a lot of noise and they are not usually so well defined, there can be some associated error. With the set limits for minima, in all cases much smaller than for maxima, this accuracy is improved trying to make it close to the $1/f_s$ limit.

4.2.2. Characterization of the impedance first derivative

Another signal that is important to characterize is the first derivative of IPG, ICG and PPG signal. As it has been explained in the theoretical part of the work, the first derivative is important to find bioparameters such as the stroke volume. In our case, the points of interest that we want to find in first derivative will be the B, E and X. The corresponding algorithm is attached in the appendix A.3 and consists of the following steps.

Impedance signal characterization: The associated impedance of the signal to be processed is characterized using our maxima and minima finding function, just to obtain the locations of the minima of the impedance signal.

B points associated: As the B point of the derivative equals the minima of the impedance signal, the indexes of the minima are taken and used to find the associated amplitude of the B points. To ensure the B points correspond to zeros in the first derivative, a condition will make all non-zero B points go the closer zero. This will be used when working with the analogical derivative.

Finding of the E and X: Knowing now that the E and X point are the corresponding maxima and minima of the derivative of the impedance, the same method for minima and maxima of the impedance will be performed. For each B point index will be set a pair of limits, and both the maximum and minimum of the range will be found, thus obtaining the E and X point.

Setting the limits: After an inspection of the impedance derivative behavior, both E and X point are always found between the indexes of the minimum and maximum of the impedance. Thus, for the E point, the indexes of the minima will be used as the lower limit and the indexes of the maxima will be used as the upper limit. For the X points, the indexes of impedance maxima will be the lower limits and the maxima indexes plus $0.2 \cdot f_s$ will act as the upper limit. The corresponding limits are shown in figure 4.8.

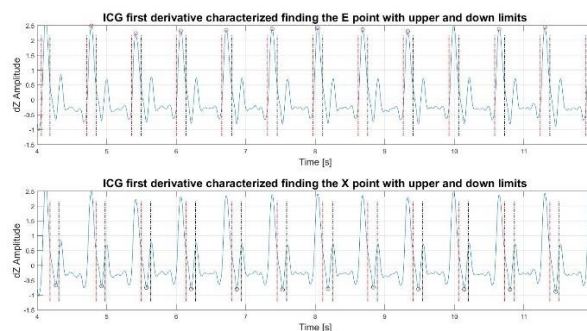


Figure 4.8. Impedance derivative with the limits corresponding to both the E and X points of the signal.

As it can be seen, each limit fits perfectly the relative position of both E and X point. Finally, using this algorithm one obtains the final signal characterized with the three points of interest.

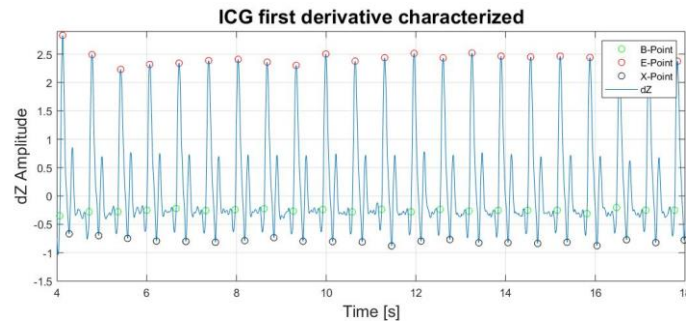


Figure 4.9. Impedance first derivative with the characteristic points.

4.2.2. Integration of the signal and the pulse wave average form

The mean integration of the signal will be considered as a parameter of interest to be found. Another important result is the average behavior of the pulse wave, meaning that an average between all the waves of each signal will be performed to obtain an approximate average form. To integrate every wave of the signal, each one will be taken separately and the corresponding minimum value will be set to zero, either the minimum is negative or positive.

When talking about the average pulse wave form, a matrix will be created to store each wave corresponding data in different rows. Once all pulse waves are stored, only the ones larger than the mean length associated to the wave pulse will be considered to compute the average signal.

To do so, an algorithm was performed, attached in the Appendix A.4, and consists in the following steps:

Impedance signal characterization: The associated impedance of the signal to be processed is characterized using our maxima and minima finding function.

Mean length of a pulse wave and matrix generation: A mean of the difference of the minima indexes of the impedance signal is performed to obtain an approximate average length of the pulse wave. A matrix is created to store each pulse wave in a row.

Each Wave Pulse Integration: A loop is generated that takes the signal from one minimum index to the following one, thus obtaining each pulse wave separately. The minimum value of the wave is set to zero. Then the `trapz()` function of Matlab is used to obtain the total integration of the corresponding pulse wave. The wave values will be stored in the matrix.

Average of the Integration and the Pulse Wave performed: At the end, the mean of all the corresponding integrations for each wave are performed. To obtain the average form, the sum of the pulse waves that are larger than the mean length will be computed.

4.3. Computation of bioparameters of interest.

Once all the signals have been characterized, some final algorithms were developed to obtain the wanted parameters. Some of them were easy, as they were directly obtained

applying some short formulas to the results of some already done algorithm or working directly with the results of the algorithms.

Arrival Time: It is found making directly the difference between the QRS ECG peak index and the index of minima of the IPG, ICG or PPG signals. An average can be performed using all arrival times obtained for each pulse wave.

Time between QRS peak and maxima of a wave pulse: The same steps are performed to obtain this second parameter. In this case, the difference is performed between the QRS ECG peaks position and the indexes of the maxima of the IPG, ICG and PPG signals.

Slope of the IPG between the minima and the maxima: The slope between maxima and minima of ICG; IPG and PPG signals is directly computed performing the difference between the maxima and minima values of the signal and then it is divided by the difference of their associated indexes.

Integration of the signal: The integration is directly obtained calling the integration method already explained in the subset 4.2.2 and added in the appendix A.4.

4.4. Model to be applied.

A final Matlab function will be generated to characterize the first derivative of the impedance signal and use the characteristic points to obtain the Stroke Volume. This function will consist of two main parts:

Characterization of the Signal: Basically, once the signal is obtained, the ECG, IPG and first derivative will be all characterized calling the required functions.

Approximation of the Stroke Volume: Once obtained all the characteristic points, the required variables to compute the stroke volume value are computed for each pulse wave:

t_{ejec} : It is obtained calculating the difference between the indexes of both X and B point for each pulse wave and dividing by the sampling frequency.

$\frac{dZ}{dt_{max}}$: It is directly obtained as the value of the E point.

Then there are two different ways to obtain the final Stroke Volume.

1. The corresponding Stroke Volume for the characterization points for each pulse wave is computed and the mean of all these Stroke Volume values is then calculated.
2. The mean for each variable is computed and then the corresponding final Stroke Volume is obtained applying directly the formula (3).

Both ways give quite comparable results and the second one will be the one to be applied.

4.4.1 Study of the sensitivity of each parameter to changes

When computing the associated propagation error of the used equation to obtain the Stroke Volume, one can easily obtain it from the general equation.

$$\frac{\Delta SV}{SV} = \left| \frac{\frac{\partial SV}{\partial t_{ejec}} \cdot t_{ejec}}{SV} \left(\frac{\Delta t_{ejec}}{t_{ejec}} \right) \right| + \left| \frac{\frac{\partial SV}{\partial Z_0} \cdot Z_0}{SV} \left(\frac{\Delta Z_0}{Z_0} \right) \right| + \left| \frac{\frac{\partial SV}{\partial \frac{dZ}{dt_{max}}} \cdot \frac{dZ}{dt_{max}}}{SV} \left(\frac{\Delta \frac{dZ}{dt_{max}}}{\frac{dZ}{dt_{max}}} \right) \right| \quad (14)$$

Where SV is the equation used to compute the approximation of the Stroke Volume and just three variables are considered as possible sources of errors: t_{ejec} , Z_0 and dZ/dt_{max} . As it can be seen in the corresponding propagation error equation 15, while a relative error of x in Z_0 and dZ/dt_{max} would suppose a $\frac{x}{2}$ relative error in the stroke volume value, the t_{ejec} would produce an error of x . Therefore, the time variable is the one that can produce a bigger error when computing an approximation of the stroke volume.

$$\frac{\Delta SV}{SV} = \left| \frac{\Delta t_{ejec}}{t_{ejec}} \right| + \left| -\frac{1}{2} \frac{\Delta Z_0}{Z_0} \right| + \left| \frac{1}{2} \frac{\frac{\Delta dZ}{dt}}{\frac{dZ}{dt}} \right| \quad (15)$$

CHAPTER 5

HARDWARE DEVELOPMENT

The main idea is to develop a device capable of acquiring accurate ECG, IPG, PPG and the basal impedance (Z_0) signals with their corresponding frequency ranges and be able to transmit and process all the information obtained in a computer. The design of the device would look as follows:

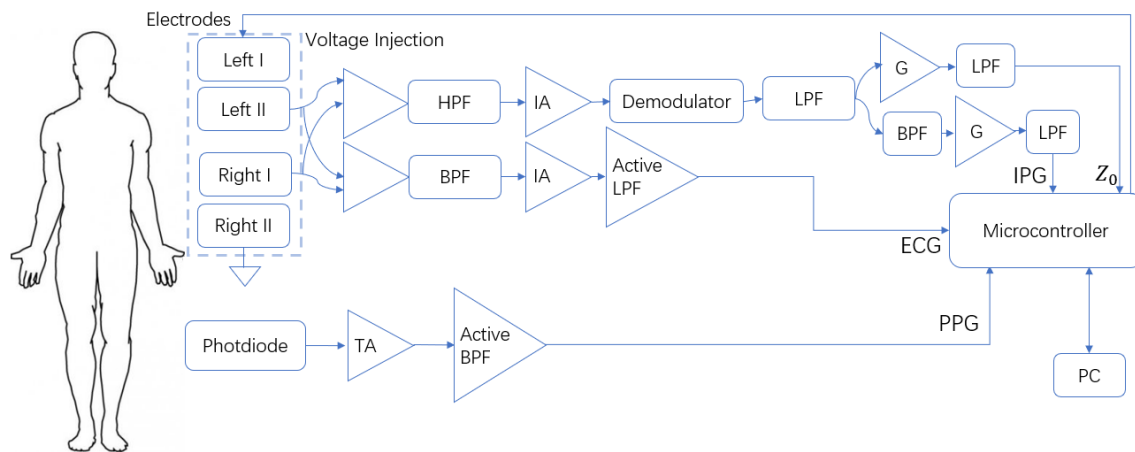


Figure 5.1. Main Schema of the hardware to be developed.

Basically, the schema starts with the four electrodes meant to measure the IPG and ECG signal, that will be placed in the spot of interest. One electrode of each pair is used to acquire the signals while the remaining two are used to inject voltage and as a reference terminal. A photodiode device can be placed as well on the subject, just to obtain the corresponding PPG signal. All these signals will be processed and undergo different filters and amplifiers, to go at the end to the Analog to Digital Converter (ADC) of the microcontroller which will be connected to a PC or some device, thus allowing us to obtain the signals.

5.1. System Specifications

The injection frequency has been selected optimally to eliminate interferences while being reasonable to implement and not overpassing the value of 1mA. The injection current will be of 200 μ A. The microcontroller board was chosen to acquire analogical signals with at least a resolution of 16 bits. The data acquisition device is the USB – 1608FS-Plus which can perform simultaneous sampling of 8 analog inputs [26]. The sampling frequency will usually be around the 1000 Hz. A portable battery of 25000 mAh is used to ensure a comfortable portability and a long usage life without having to recharge so often.

Electrode Type	Dry electrodes, AgCl
ECG frequency range	0.5 - 100 Hz
IPG frequency range	0.05 - 20 Hz
PPG frequency range	0.05 - 20 Hz
Injection Frequency	200 μA
Injection current	10 kHz
ADC resolution	16-bit
Data Acquisition	USB-UART
Power	Li-ion Battery (25000mAh)

Table 5. Hardware Specifications.

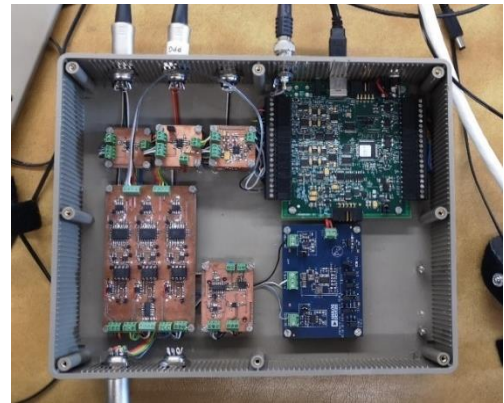


Figure 5.2. Developed hardware.

5.2. Required electronic elements

5.2.1. Low Pass Sallen-Key Filter

The Sallen-Key configuration was first introduced in 1955. The basic configuration as a low pass active filter is shown in the figure 5.3.

It is widely used, as its circuit configuration shows the least dependence of filter performance on the operational amplifier. All the second order filters used in the hardware development belong to the Sallen-Key family.

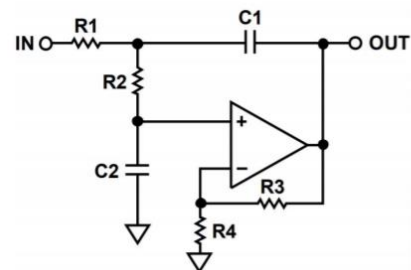


Figure 5.3. Sallen-Key low pass filter.

5.2.2. Amplifiers

Differential amplifiers are a type of electronic amplifier that increase the amplitude of the difference between two input voltages signals, not considering their individual values. Thus, suppressing any voltage common in both input signals. Hence a differential amplifier is used to amplify only the potential difference between the two points of the body that are being measured.

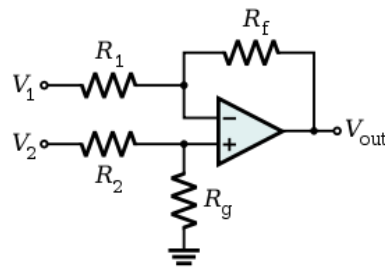


Figure 5.4. A classical differential amplifier.

When using differential amplifiers, the typical interferences such as the electrical wiring in the building, placed around the 50 or 60 Hz, or the muscular noise are cancelled out, as the same interferences are present in both input signals. For electrical safety, differential amplifiers must have an isolated signal ground.

An instrumentation amplifier (IA) comes under the family of differential amplifiers. It is a closed loop gain circuit with different inputs signals and just an only output signal. Usually the input signals present high impedances while input bias current are quite low. The gain is set independently from the input signal.

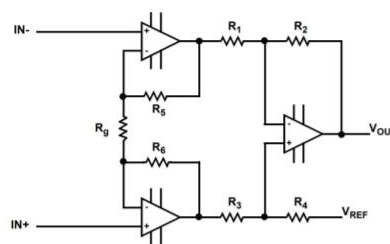


Figure 5.5. Classic instrumentation amplifier circuit.

The AD8426 IA was chosen for the application, as it supports a wide range of gain from 1 to 1000 and a bandwidth product of 1 MHz.

5.2.4. AM Demodulation

Amplitude Modulation (AM) is a technique to transmit human voice over Radio waves. In the amplitude modulation, the amplitude of the carrier changes according to the amplitude of the input signal. This same effect can be observed in the human body while a frequency is injected, the impedance changes in the body modulate the amplitude of the injected frequency. Therefore, a demodulation technique is required to obtain the wanted variation of impedance and the basal component. In our case, a switch and a low pass filter will be used to act as a demodulator.

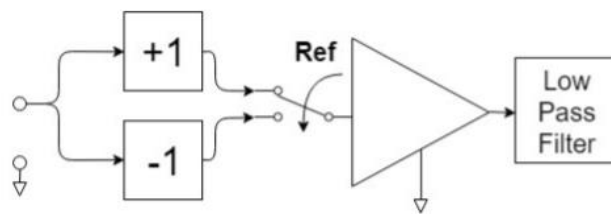


Figure 5.6. Switching demodulator block circuit.

Basically, the switch is controlled by a comparator, which compares the signal to a reference voltage. When the signal is higher than the reference, the signal remains the same and passes to the operational amplifier, while when the signal is lower, the inverse of the input signal passes.

5.3. Electrocardiograph

The ECG signal is first measured using four different electrodes. Then it passes to the differential amplifier after undergoing a bandpass filter, having a Gain of $G=183$.

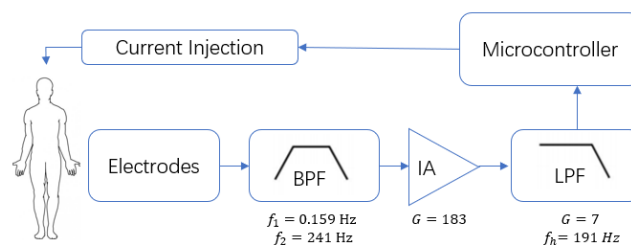


Figure 5.7. Electrocardiograph block diagram.

The frequency filter limits have been chosen to ensure there would not be any waveform distortion in the acquired signal and make the signal smoother. Once having passed

through the Instrumental Amplifier, there would not be any need to add more filters. However, as ECG and IPG signals are acquired simultaneously, the carrier frequency of IPG is a strong interfering signal for ECG and therefore, a second low pass filter is applied to erase this interference.

5.4. Impedance Plethysmograph

The acquisition of the IPG signal is quite more complicated compared to obtaining ECG.

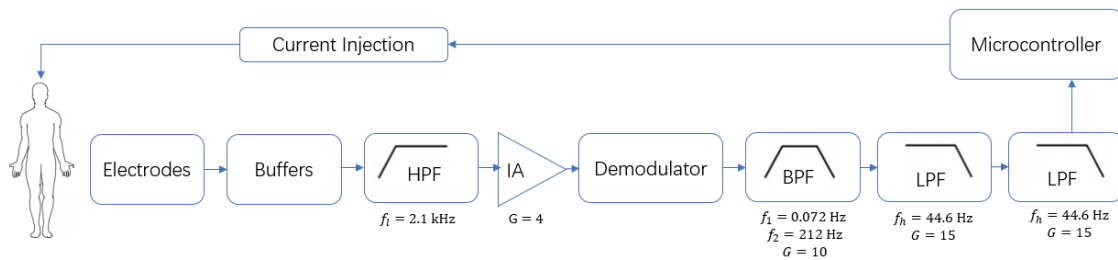


Figure 5.8. Impedance Plethysmograph block diagram.

The electrodes are the same used in the electrocardiograph circuit, but a new set of buffers are used to avoid a loading effect on the filters. After the buffers, a differential high pass filter is set around 2 kHz to eliminate signals which are not needed like electrocardiogram and electromyograph, as the IPG signal is placed at 10 kHz. After that, an operational amplifier with a gain of 4 is applied and then undergoes through demodulation, which has already been explained in the subset 5.2.4 and allows to obtain the signal of interest from the modulated output signal. After the demodulation, a first band pass is applied just to erase the continuous impedance signal (basal impedance Z_0 of the body). After obtaining the IPG signal, two more Sallen-Key filters are applied which provide additional gain and a smoother signal. To obtain the basal impedance, after the demodulation an amplifier followed by a low pass filter are used to erase the IPG signal and obtain just the Z_0 value.

5.5. Photoplethysmograph

The main design consists of a LED reflecting light over the skin and a photodiode to convert the light into current. Then a transimpedance amplifier will be used to convert the current to a readable voltage. After that, a pair of operational amplifiers convert this

current into voltage and provide an amplification to be converted to digitally by the ADC. The used photosensor will be SFH-7070 [27].

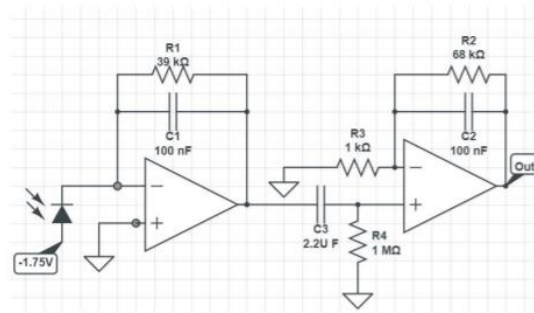


Figure 5.9. Photoplethysmograph Circuit Design.

The required amplification is split in two different stages. First a transimpedance amplifier is used and then applying another voltage amplifier as a bandpass filter later. The photodiode here is used in the photoconductive mode.

5.7. Power Supply

Just to obtain an electrical isolated device, a battery power supply was mandatory. A li-ion battery with 25000 mAh capacity is used due its ability to recharge, big supply and comfortability. The average voltage of the battery is around 5 V, being transformed in the circuit first to ± 15 V using a commutated elevator regulator and then to ± 12 V using a linear regulator that allows to erase the noise added during the first amplification of voltage.

5.8. Device Usage

When the device was completely developed, some experimental usage was performed just to confirm the obtained signals were good enough.

Once confirmed the acquired signals were accurate, some new positions such as the foot to foot or hand to hand measures were performed in a weighing scale, demonstrating how a normal device everyone has at home can be used to perform daily or routine monitoring of the cardiovascular system.



Figure 5.10. Using a weighing scale to perform foot to foot and hand to hand IPG measures.

6.1. Variability of the signals

The main objective during the first weeks of working was to observe the changes on the behavior of the IPG and understand how these signals evolved when propagating through the body, changing their associated bioparameters. Two main hypotheses were made regarding this evolution of the signals:

1. The further the signal spot from the heart is, the smaller the integral and the slope of the pulse wave, because a smaller amount of blood arrives to the spot.
2. The further the signal spot from the heart is, the bigger the times between both minima and maxima from the QRS peak are.

To confirm or reject both hypotheses, the four parameters described in the subset 4.3 were obtained from the signals of 11 different subjects. The resulting parameters are shown in the tables of the appendix B.

As it can be seen in the tables, both hypotheses were correct. As the change of impedance is directly related to the change of the volume of the arteries, the smaller the vessels are, the less the volume will change. Hence having a smaller integral and slope. On the other hand, as minima are related with the arrival of blood to the spot and maxima with the leaving, the further from the heart we measure, the more time the blood requires to arrive to the measure spot. Even though there are some cases where this order is altered, the main pattern follows the logics raised in both hypothesis.

Regarding the PPG signals, the only parameters that can be compared are the corresponding times. As this signal comes from a different technique, the corresponding amplitude is much bigger, presenting huge integrals and slopes. When observing both times (from maxima and minima), they follow the same logic, being always the biggest values as the PPG measure is performed in the left index finger.

Once both hypotheses were fulfilled, the next natural question was to know how the behavior of these signals evolved when propagating throughout the body. As vessels change the diameter and many other factors change, it is logical to think that the behavior of the signals will be altered as well.

To understand a bit how these signals evolve, the average form of each pulse wave from the six upper part of the body measures (Z1, Z2, Z3, Z4, Z5, Z7) are computed. Thus, the effect that arms have on these signals can be easily observed. In the figure 6.1 the corresponding graphs of 4 different subjects are attached.

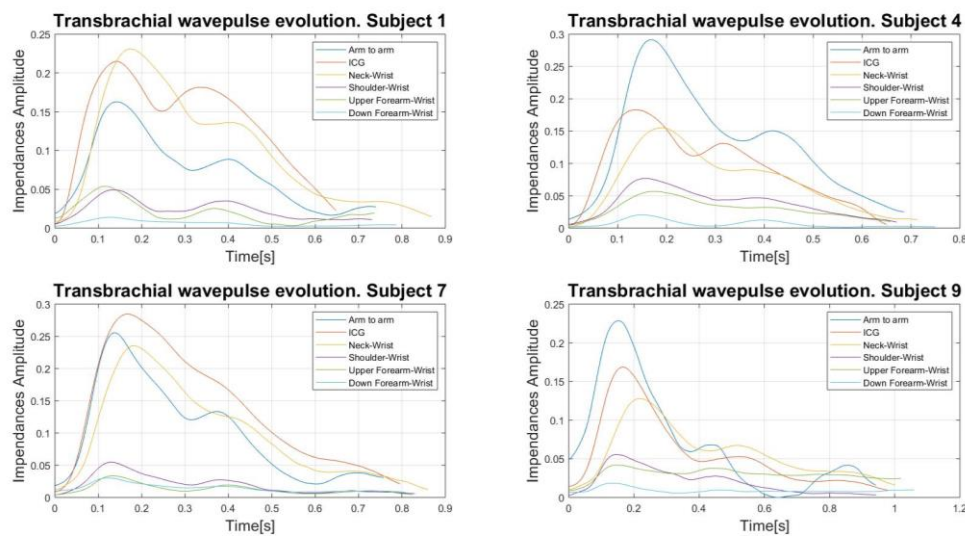


Figure 6.1. Transbrachial evolution of the pulse wave for 4 different subjects.

As it was expected, the signal amplitude decreases as it gets further from the heart. It is coherent with the first hypothesis that has been confirmed. However, the change of amplitude for each measure changes individually for each subject, not presenting any common pattern for all subjects.

An interesting fact to observe that this is not always fulfilled when comparing both ICG (Z1) and arm to arm (Z7) signals, or when considering the Neck (Z2) signal as well. It is important to consider that the impedance signals are the result of integrating the impedance of the whole zone remaining between the both pair of electrodes. Thus, the bigger the zone between both electrodes, the bigger the signal should be. Again, this is coherent with the hypotheses that had been first made, as the bigger the zone

integrated, the more changes in volume its vessels will suffer and the bigger amplitude the impedance signal should present.

Despite this, the ICG (Z1), the arm to arm (Z7) and the neck (Z2) signals are the only signals that switch the order depending on the subject. Thus, one can conclude that each individual presents different characteristics of the cardiovascular system, having some people bigger changes in the aorta and other individuals bigger average changes from one arm to the other arm path. Thus, this will depend on the own cardiovascular characteristics each subject presents.

A second study was performed, in this case considering the time when the signals started to increase. This means, computing how much time was needed to make the pressure wave propagate from the heart to the spot that was being measured. The same four graphs can be observed again in the figure 6.2, this case considering the delay between the different signals.

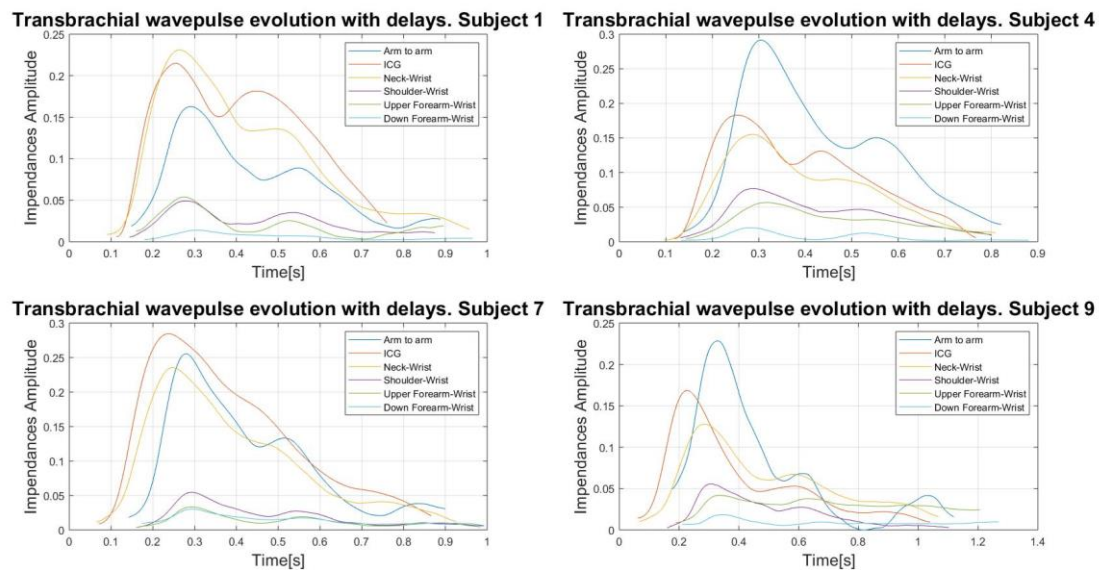


Figure 6.2. Transbrachial evolution with delays of the Wave Pulse for 4 different subjects.

As it can be seen, the first signal to start increasing corresponds always to the ICG (Z1), happening this with the full set of subjects. The rest of signals, start following the same logic used before, being the further signals the ones that increase the latest. Some exceptions happen with smaller signals, that start almost at the same time, being it

explained due their physical closeness, as the lower arm measures are near between them and therefore, present similar delays.

There is a signal that seems to break this whole logic. As the arm to arm (Z7) integrates all the signals present from one hand to the other, it was thought to measure the blood ejection from the heart. Therefore, it should start almost simultaneously to the ICG (Z1) signal. Making a fast glance at the figure 6.2 again, the arm to arm signal starts quite later and repeats this behavior in all the subjects. The main reason is that while the Neck (Z2) and ICG (Z1) signal measure the first artery getting the blood ejected from the heart (the aorta artery travelling down the chest), the arm to arm (Z7) measures the second artery that drives this blood to the arms (subclavian artery). Hence the arm to arm (Z7) signal starts relatively close to the Z3, Z4 and Z5 signals while the Neck (Z2) and ICG (Z1) start almost simultaneously.

To confirm this last fact, two local measures were taken. In both measures the first two electrodes were placed in the chest, and the second pair was placed in the shoulder in a first place to integrate the subclavian artery, while in the second place the aorta artery was measured placing them in the down part of the chest. Following the logic explained before, the first signal should start later following the same behavior as the arm to arm (Z7) signal, while the second signal should start earlier resembling the ICG (Z1) behavior. It is clearly confirmed, as it can be seen in the graph 6.3 attached bellow.

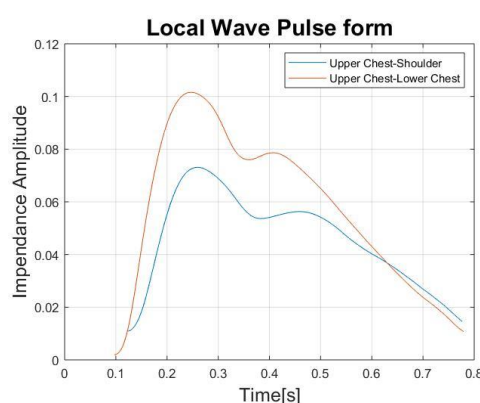


Figure 6.3. In Blue the Upper-Chest Shoulder measure to integrate the subclavian artery. In orange the Upper-Chest Lower-Chest measure to integrate the aorta.

Another interesting fact that can be clearly confirmed, is the widen effect the limbs have on the pulse wave. When measuring the mean length of the pulse wave for each signal,

the ICG (Z1) always present the smaller mean length while the lower arm signals presents the widest pulse wave. This can be easily explained considering that smaller arteries tend to present smaller velocities, thus presenting a slower change of pressure.

A last worth considering fact is the presence of different peaks in the IPG signals. As it has been explained in the theoretical part, there are three main peaks: Due the ejection of blood, due the reflection and due the valve closure. It is curious to observe that while the ICG (Z1) signal tends to present the three peaks not really pronounced or two main peaks and a third one quite small, the arm to arm signal and the lower ones tend to present three main peaks, distinguishable between them.

The main cause of this is the difference of amplitude between the signals. While the ICG (Z1) signal measures the aorta, which presents a huge amount of blood, the first peak is really pronounced as the arrival of the blood ejected from the heart presents a large change of volume. Therefore, any other change is hardly noticeable, as the starting amplitude has already changed a lot. It is curious to observe that while the reflection peak is hard to notice for all subjects, the closure of the aortic valve depends of the subject, having many of them a no-noticeable change while others present a huge change. This can be related with the flexibility of the arteries, having a bigger change of pressure due the aorta valve closure when the arteries are more flexible.

However, as the lower signals measure tiny arteries which present minor changes of volume, any change in the arteries produces a huge change of the impedance amplitude. Meaning that the first peak is always the bigger, as the amount of blood changes a lot the volume of the arteries but presenting distinguishable peaks as the other changes produce a noticeable change of amplitude as well.

However, a final question comes in mind when considering the case of the arm to arm (Z7) measure. It presents a huge amplitude, but the three peaks are noticeable. This is explained because it is an integration of all the local signals going from one hand to the other. To prove it, some local measures were performed. A first ICG signal was performed, and then the second pair of electrodes which initially where placed in the neck, were placed in different spots of the arm. Thus, integrating at the end from the left

thoracic side of the body to the left arm. The main idea was to understand if when integrating these local measures in the lower arm, the third peak is more visible and thus gains importance. As it can be seen in the figure 6.4, when integrating

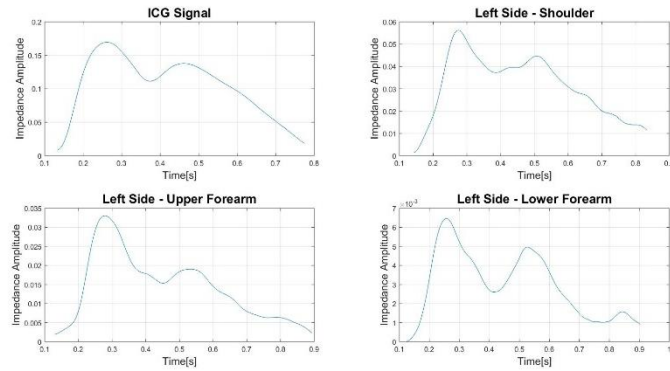


Figure 6.4. Local ICG signals evolution.

the whole arm, the three peaks are more distinguishable between them than when just integrating the ICG signal.

6.2. Obtention of the Stroke Volume from IPG signals

The main and final goal was to perform an approximation of the Stroke Volume from different IPG signals. The main idea was to apply the formula found in the equation (3) and see how close to the real Stroke Volume are the obtained values. Applying this formula, the first raw approximation was obtained.

Subject	Real SV [mL]	Arm to Arm [mL]	Leg to Leg [mL]	Upper Arm [mL]	Upper Forearm [mL]	Lower Forearm [mL]
S1	69.28	55.93	48.20	46.01	58.96	51.67
S2	65.33	49.15	41.33	32.57	38.32	35.66
S3	44.89	67.79	45.18	58.22	42.01	37.82
S4	54.47	71.93	43.90	50.69	65.12	68.37
S5	47.76	54.11	49.57	55.08	47.51	49.66
S6	74.93	57.20	41.30	52.87	44.01	57.50
S7	63.87	47.27	32.71	40.67	42.47	37.72
S8	44.07	66.31	39.80	43.96	43.93	46.11
S9	67.23	62.89	47.82	52.06	50.59	45.69
S10	84.70	67.79	63.43	56.72	63.15	62.27
S11	45.95	54.66	38.12	68.53	52.44	41.11

Table 6. First approximated values of the Stroke Volume from IPG measures.

Once this first data was obtained, each approximated SV was divided by the real SV value of the corresponding subject, just to see which factor was between both numbers. It was surprising to find that for every subject, this coefficient was quite constant, being always contained in a small range of values. However, if observing the coefficients of the same

measure for different subjects, it is clear there is no correlation and that the main influence is the subject itself and not the spot of the measure.

Subject	Arm to Arm	Leg to Leg	Upper Arm	Upper Forearm	Lower Forearm	Mean Coefficient
S1	0.81	0.70	0.66	0.85	0.75	0.75
S2	0.75	0.63	0.50	0.59	0.55	0.60
S3	1.51	1.01	1.30	0.94	0.84	1.12
S4	1.32	0.81	0.93	1.20	1.26	1.10
S5	1.13	1.04	1.15	0.99	1.04	1.07
S6	0.76	0.55	0.71	0.59	0.77	0.68
S7	0.74	0.51	0.64	0.67	0.59	0.63
S8	1.50	0.90	1.00	1.00	1.05	1.09
S9	0.94	0.71	0.77	0.75	0.68	0.77
S10	0.80	0.75	0.67	0.75	0.74	0.74
S11	1.19	0.83	1.49	1.14	0.89	1.11

Table 7. Propagation coefficient for each subject and measure.

Making an average coefficient of each subject, it can be considered as a constant coefficient of propagation, meaning that for every person the pulse wave propagates approximately constant throughout the body. Dividing now each subject value for the Mean coefficient, a better approximation of the Stroke Volume was obtained.

Subject	Real SV [mL]	Arm to Arm [mL]	Leg to Leg [mL]	Upper Arm [mL]	Upper Forearm [mL]	Lower Forearm [mL]
S1	69.28	74.30	64.02	61.12	78.33	68.64
S2	65.33	81.49	68.52	54.00	63.54	59.13
S3	44.89	60.62	40.40	52.07	37.57	33.82
S4	54.47	65.29	39.85	46.01	59.11	62.06
S5	47.76	50.49	46.25	51.39	44.33	46.33
S6	74.93	84.74	61.19	78.32	65.21	85.19
S7	63.87	75.16	52.00	64.67	67.53	59.97
S8	44.07	60.86	36.52	40.35	40.32	42.32
S9	67.23	81.61	62.05	67.55	65.65	59.28
S10	84.70	91.62	85.71	76.66	85.34	84.16
S11	45.95	49.27	34.36	61.79	47.27	37.06

Table 8. Approximated Stroke Volume values after calibrating with the propagatin coefficient for each subject.

Plotting now the data in a dispersion graphic, one can observe the huge improvement the calibration factor (personalization) produces in the raw data. From a correlation factor of $r=0.16$, a final data with a correlation factor of $r=0.91$ was obtained, just dividing each SV value by the personal propagating coefficient.

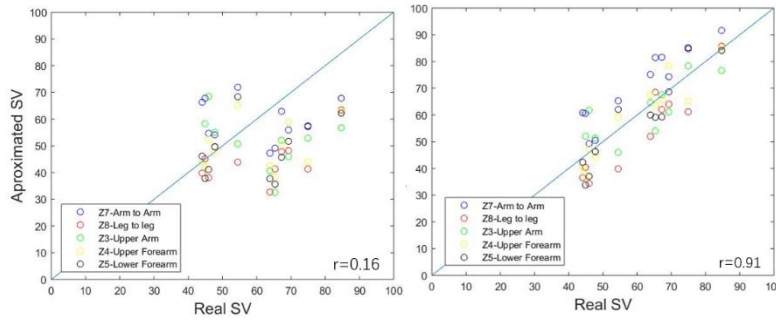


Figure 6.5. On the left, the dispersion graph of the raw data with a correlation value of $r = 0.16$. On the right, the dispersion graph of the post-calibration and readjustment data with a correlation value of $r = 0.91$.

However, when observing closely the data, one can realize that the Stroke Volume values that were bigger, were obtained from signals where the three variables $\frac{dZ}{dt}$, ΔZ and t_{ejec} presented bigger values as well. Therefore, one could think that when the signals presented larger values, the SV could be affected and resulted in worse results. A new corrective coefficient was applied just to see if there was an improvement of the results. Three different parameters were considered:

$$a = \frac{dZ}{dt} \cdot \Delta Z \cdot t_{ejec} \quad (16) \qquad b = \Delta Z \cdot t_{ejec} \quad (17) \qquad c = \Delta Z \quad (18)$$

Just to know which one of the three would fit the most, the corrective coefficient between the parameters and each signal SV values was performed. As it was expected, the b parameter presented the higher correlation values for all signal.

	a	b	c
Z3	0.35	0.50	0.21
Z4	0.71	0.74	0.65
Z5	0.25	0.42	0.26
Z7	0.38	0.54	0.31
Z8	0.74	0.75	0.65

Table 9. Correlation between the approximated stroke volume values and each corrective parameter.

Physically, the b constant can be considered as the area under the impedance signal while the blood is still arriving to the spot. It is the area of the main peak of the IPG signal, which contains the most information as reflects the arrival of the blood ejected. Therefore, when the signals present a bigger area defined by

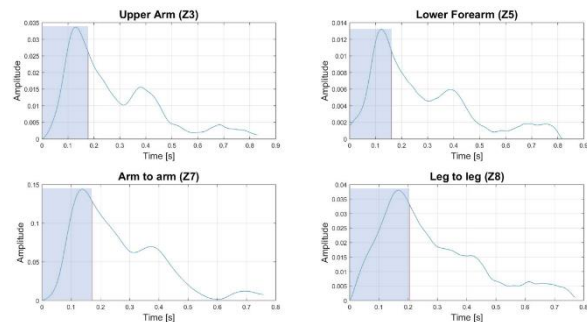


Figure 6.6. Main area defined by ejection time and the amplitude of the impedance signal.

both ΔZ and t_{ejec} , the approximation of the stroke volume tends to increase.

Once the b parameter was chosen, a function was required. This function had to fulfill some conditions. First, the propagation coefficient should not be affected, meaning that the SV values should be multiplied or divided by some values near the unity. In addition, this corrective parameter should consider that the bigger the value was, the more the SV value should decrease. Two distinct functions were designed:

$$f(x) = SV \cdot (1 - x) \quad (19) \quad f(x) = SV/(1 + x) \quad (20)$$

Thus, obtaining two new SV functions.

$$SV_A = 32 \cdot W^{1.02} \sqrt{\frac{dZ/dt}{Z_0}} \cdot (1 - \Delta Z \cdot t_{ejec}) \quad (21) \quad SV_B = 32 \cdot W^{1.02} \frac{\sqrt{\frac{dZ/dt}{Z_0}}}{1 + \Delta Z \cdot t_{ejec}} \quad (22)$$

Both functions resulted in similar improvements, as it was already expected. The main reason was that the SV_A correction is the first order Taylor expansion of the SV_B , having thus an approximate similar effect in the SV values. However, the A function was the one which improved the most our SV values.

Subject	Real SV [mL]	Arm to Arm [mL]	Leg to Leg [mL]	Upper Arm [mL]	Upper Forearm [mL]	Lower Forearm [mL]
S1	69.28	73.48	63.87	61.29	78.54	69.23
S2	65.33	80.38	68.00	54.32	64.13	59.85
S3	44.89	59.01	40.44	52.56	38.07	34.39
S4	54.47	63.56	39.70	46.27	59.64	63.15
S5	47.76	49.89	45.94	51.45	44.70	46.80
S6	74.93	83.36	60.68	78.76	65.87	85.98
S7	63.87	73.14	51.86	65.16	68.35	60.81
S8	44.07	59.68	36.45	40.59	40.80	42.85
S9	67.23	79.90	61.58	68.16	66.44	60.06
S10	84.70	89.87	84.01	77.45	86.48	85.68
S11	45.95	49.07	34.18	61.55	47.58	37.38

Table 10. Final approximated Stroke Volume values after calibration and readjustment.

Now plotting the dispersion graph for each spot of measure, one can see the linear behavior that final results present and the big correlation constant they present. It is interesting to observe how the arm to arm signal usually tends to give bigger values than the real ones while the leg to leg signals tends to give smaller ones. The other three signals present both bigger and smaller values indistinctively.

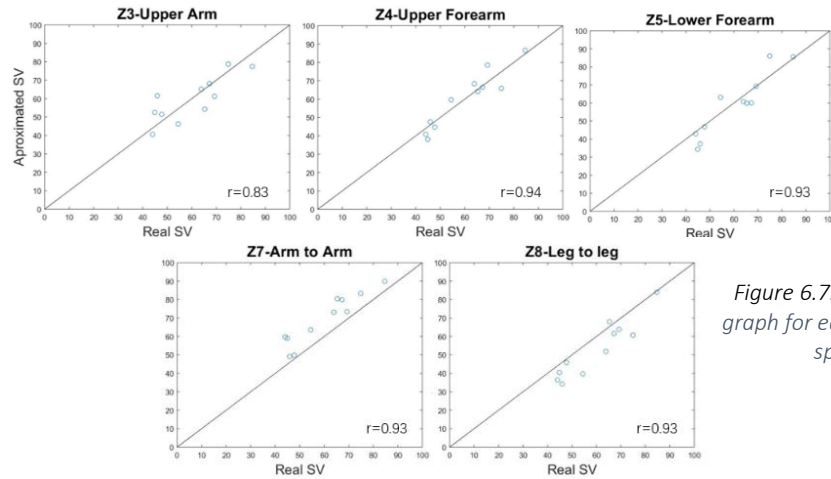


Figure 6.7. Dispersion graph for each measure spot.

This entire process was repeated using the actual area contained under the impedance curve and delimited by the $t_{e_{jec}}$ variable, and not using the approximated area $\Delta Z \cdot t_{e_{jec}}$. However, no further improvement was observed, obtaining approximately the same result. The mean error for each subject and measure is attached in the following tables.

Subject	Mean Error (%)
S1	7.77
S2	10.84
S3	19.41
S4	16.86
S5	4.88
S6	12.44
S7	9.43
S8	14.16
S9	8.09
S10	3.75
S11	17.71

Measure	Mean Error (%)
Z7	15,88
Z8	12,97
Z3	11,56
Z4	7,24
Z5	9,33

Table 11. Mean error by measure spot.

Table 12. Mean error by subject.

One can easily conclude that an improvement from the existing found studies where the SV value was approximated from other spots, as the correlation coefficient ranged between 0.70 and 0.85 and the mean error was above 20%, as it can be observed in the following papers results. [12] [20]

CONCLUSIONS AND FUTURE PERSPECTIVES

A new equation model to obtain the stroke volume from different IPG signals has been obtained, presenting better results than the ones that had been used so far. The studies found in the bibliographical research presented correlations values between the $r = 0.7$ and $r=0.85$ and mean errors above the 20%, having achieved during this thesis a correlations values from $r = 0.83$ to $r=0.94$ and mean errors between the 10-20%.

Finally, there are four main conclusions that one can easily extract from this whole thesis.

1. The evolution of the pulse wave throughout the body was as expected, following the hypotheses that we already had formulated and the logic that was expected to be found.
2. The propagation of the pulse wave signal throughout the body depends on each individual. This parameter remains almost the same for every subject, making it possible to approximate the SV value from any spot of the body.
3. IPG signals can be used to monitor the cardiovascular system instead of the commonly used ICG signal. Meaning that the same information can be extracted from IPG measures in other spots much more comfortable.
4. A versatile and cheap device can be developed to allow both patients and doctors to monitor the cardiovascular system using easier measure spots such as the foot to foot in weighing scales.

As this thesis ends, there is a future research that can be done. To begin, a new study in l'Hospital Clinic will be started to validate the obtained results with a bigger population and an important improvement for the new study will be the possibility to work with people suffering from cardiovascular problems.

On the other hand, one of the most surprising findings was to demonstrate there was a propagation constant that vary just a little for everyone, being then the subject a more important influence on this parameter rather than the spot where the measure is performed itself. The next natural question should be how this parameter changes with time (in case it does) and what does imply a change of this parameter. In our case, we have found a repeatability for this constant for some subjects during different weeks, however, for lack of time no more study of this evolution was able to be performed.

Appendix A

CODES AND SCRIPTS

A.1 Pan-Tompkins Algorithm

```
function [IBP,MeanRR] = PTfun(ECG,fs,ks)

%% ===== PREPARATION OF THE SIGNAL=====%%
%% ===== Filtering( 5-15 Hz)=====%%
f1=5; % cutoff low frequency
f2=15; % cutoff frequency to discard high frequency
noise
Wn=[f1 f2]*2/fs; % cutt off based on fs
N = 3; % order of 3 less processing
[a,b] = butter(N,Wn); % bandpass filtering
ECG_BP= filtfilt(a,b,ECG);

%% ===== Derivative Filter =====%%
b = [1 2 0 -2 -1].*(1/8)*fs; %The derivative filter is applied.
ECG_D = filtfilt(b,1,ECG_BP);

%%=====Squaring=====%%
ECG_S = ECG_D.^2; %The squared signal is generated

%% =====Moving Windows =====%%
ECG_W = conv(ECG_S ,ones(1 ,round(0.150*fs))/round(0.150*fs));
x = [1:length(ECG)]; tvec = x/fs; %A time vector is generated.

%% =====ALGORITHM=====%%
%% =====FIDUCIAL MARK=====%%
%The QRS peaks must separated between them at least with 200 ms.
%The peaks in the windowed signal are close to the real ones.
%A first selection of all the peaks in the window signal will
%be done, then just the real ones will be stored.
[peaksW,indexW] = findpeaks(ECG_W,'MINPEAKDISTANCE',round(0.2*fs));
LpeaksW = length(peaksW);

%% =====INICIALIZATION=====%%
%% Windows Integrated Signal
%Void vectors are generated to store the evolution of thresholds.
SigPeakW = mean(ECG_W(1:fs))/2;
SigPeakW_vec = zeros(1,LpeaksW);
NoiPeakW = mean(ECG_W(1:fs))/3;
NoiPeakW_vec = zeros(1,LpeaksW);
THRW = NoiPeakW + 0.25*(SigPeakW-NoiPeakW);
THRW_vec = zeros(1,LpeaksW); THRW_Noise = 0.5*THRW;

%% BandPass Filtered Signal
%Void vectors are generated to store the evolution of thresholds.
SigPeakBP = mean(ECG_BP(1:fs))/2;
```

```

SigPeakBP_vec = zeros(1,LpeaksW);
NoiPeakBP = mean(ECG_BP(1:fs))/3;
NoiPeakBP_vec = zeros(1,LpeaksW);
THRBP = NoiPeakBP + 0.25*(SigPeakBP-NoiPeakBP);
THRBP_vec = zeros(1,LpeaksW);THRBP_Noise = 0.5*THRBP;

%% =====THRESHOLDS=====%%
%%Void vectors are generated to save the possible peaks
AW=[]; IW=[]; ABP=[]; IBP=[]; Aprova=[];Iprova=[];
%%A loop is generated to choose each peak of the windowed signal.
for ii = 1:LpeaksW
    %A first condition is imposed. If it is true, the peak can
    be real.
    if peaksW(ii) > THRW %The peak can be QRS
        %The index of the peak is found
        pos_peak = find(ECG_W==peaksW(ii));
        %Vectors are updated
        AW = [AW, peaksW(ii)]; IW = [IW, pos_peak];
        %The thresholds will be updated.
        SigPeakW =0.125*peaksW(ii) + 0.875*SigPeakW;

        %% Now we search for peaks in the Band Pass Filteres Signal
        %The position of the peak is normalized to the
        %filtered signal.
        pos_peak_BP = round(pos_peak*length(ECG)/length(ECG_W));
        %Now the limits where the algorithm will look for
        %the peak are set.
        bottom = max(1,(pos_peak_BP-100));
        top = min(pos_peak_BP+100, length(ECG_BP)-1);
        %A temporal variable is defined containing the range where
        %the peak must be.
        peakBP = max(ECG_BP(bottom:top));
        %Second condition. If the peak is bigger than the
        %filtered signal threshold, it can be a real peak.
        if peakBP > THRBP
            %The position of the peak is found.
            pos_peak = find(ECG_BP==peakBP);
            %The vectors are updated.
            ABP = [ABP, peakBP];IBP = [IBP, pos_peak];
            Aprova=[Aprova, peakBP];Iprova=[Iprova,pos_peak];
            SigPeakBP =0.125*peakBP + 0.875*SigPeakBP;
        else
            %If the peak is false, the noise threshold is updated
            NoiPeakBP =0.125*peakBP + 0.875*NoiPeakBP;
        end
    elseif THRW_Noise<peaksW(ii) && THRW_Noise<peaksW(ii)
        %If both conditions are fulfilled, the peak is directly noise.
        NoiPeakW =0.125*peaksW(ii) + 0.875*NoiPeakW;
    end
end
%% ===== SEARCH BACK =====%%
%%Once we have enough peaks, a mean separation is computed.
if length(AW)>9
    MeanRR = mean(diff(IW));
    %Looking for lost peaks in the windowed integrated signal.
    if (IW(end)-IW(end-1))>1.66*MeanRR
        %If the condition is fulfilled, a peak has been left behind.
        %The thresholds are decreased to be more sensitive.
        THRW = THRW/2;SigPeakW = SigPeakW/2;
        NoiPeakW = NoiPeakW/2;

        %The algorithm looks for some new peak in the region where one

```

```

%has been left behind.
peakW = max(ECG_W(IW(end-1)-500:IW(end)+500));
%If this new peak is over the threshold variable, it is real.
    if peakW > THRW/2
        %The position of the peak is found.
        pos_peak = find(ECG_W==peakW);
        %A temporal variable is generated to store the last
        %peak.
        pk_temp = AW(end); pos_temp = IW(end);
        %The last peak is erased.
        AW(end) = []; IW(end) = [];
        %The newfound peak and the last one are added.
        AW = [AW, peakW, pk_temp];
        IW = [IW, pos_peak, pos_temp];
    end

end

%Looking for lost peaks in the bandpass filtered signal.
if (IBP(end)-IBP(end-1))>1.66*MeanRR
    %If the condition is fulfilled, a peak has been left behind.
    %The thresholds are decreased by a half to be more sensitive.
    THRBP = THRBP/2; SigPeakBP = SigPeakBP/2;
    NoiPeakBP = NoiPeakBP/2;
    %The lost peak must be placed between the last peaks.
    pos_peak = (IW(end-2)+IW(end))/2;
    %The filtered signal equivalent peak must be in the
    %proportional index.
    pos_peak_BP =
    round(pos_peak*length(ECG)/length(ECG_W));
    %The peak is found directly using the max function.
    peakBP = max(ECG_BP(pos_peak_BP-400:pos_peak_BP+400));
    %If it fulfills the condition, the vectors are updated.
    if peakBP > THRBP/2
        %The position of the peak is found.
        pos_peak = find(ECG_BP==peakBP);
        %A temporal variable is found storing the last
        %peak.
        pk_temp = ABP(end); pos_temp = IBP(end);
        %The last peak is erased.
        ABP(end) = []; IBP(end) = [];
        %The vectors are updated.
        ABP = [ABP, peakBP, pk_temp];
        IBP = [IBP, pos_peak, pos_temp];
    end
end

end

end

%% ===== Detection for T Waves ===== %%
if length(IBP)>3 %The condition for T Waves is applied.
    if (IBP(end)-IBP(end-1)) <= round(0.3600*fs)
        %The slopes of the last two pulses are computed.
        Slope1 = mean(diff(ECG_BP(IBP(end)-
        round(0.075*fs):IBP(end))));
        Slope2 = mean(diff(ECG_BP(IBP(end-1)-round(0.075*fs):IBP(end-
        1))));
        if abs(Slope1) <= abs(0.5*(Slope2))
            %If the condition is fulfilled, the last peak is a T-Wave.
            IW(end) = []; AW(end) = [];
            IBP(end) = []; ABP(end) = [];
        end
    end
end

end

```

```

%The thresholds are updated.
THRW = NoiPeakW + 0.25*(SigPeakW-NoiPeakW);
THRW_Noise = 0.5*THRW;
THRBP = NoiPeakBP + 0.25*(SigPeakBP-NoiPeakBP);
THRBP_Noise = 0.5*THRBP;
%% ===== UPDATE VECTORS =====%%
SigPeakW_vec(ii) = SigPeakW;
NoiPeakW_vec(ii) = NoiPeakW;
THRW_vec(ii) = THRW;
SigPeakBP_vec(ii) = SigPeakBP;
NoiPeakBP_vec(ii) = NoiPeakBP;
THRBP_vec(ii) = THRBP;
MeanRR = mean(diff(IBP/fs));
end
end

```


A.2 Impedance Characterization

```

function[IBP,IPGmax, IPGmin, IPGmax_index,IPGmin_index] =
characterization(ECG,Z,type,fs)
%% Filtering of the signals
Fs = 2000; % Sampling Frequency (Hz)
Fn = Fs/2; % Nyquist Frequency (Hz)
Wp = [0.5 40.0]/Fn; % Passband Frequencies (Normalised)
Ws = [0.4 40.1]/Fn; % Stopband Frequencies (Normalised)
Rp = 10; % Passband Ripple (dB)
Rs = 50; % Stopband Ripple (dB)
[n,Ws] = cheb2ord(Wp,Ws,Rp,Rs); % Filter Order
[z,p,k] = cheby2(n,Rs,Ws); % Filter Design
% Convert To Second-Order-Section For Stability
[sosbp,gbp] = zp2sos(z,p,k);
tv = linspace(0, 1, length(Z))/Fs; % Time Vector (s)
Z = filtfilt(sosbp,gbp, Z);
%% The kmax variable is defined
kmax = 0.4*fs;
%% The Pan-Tompkins function is called
[IBP,MeanRR] = PTfun1_0(ECG,fs,ks);
%% Depending on the type, some different limits will be defined.
if type == 1
    kmin = (MeanRR/4)*fs; kmin = floor(kmin);
end
if type == 2
    IBP = IBP + floor(MeanRR*fs/8);
    kmin = (MeanRR/4)*fs; kmin = floor(kmin);
end
%% Loop to find both minima and maxima
IPGmax=[]; IPGmax_index=[]; IPGmin=[]; IPGmin_index=[];
%A loop to pick each QRS peak is generated.
for ii = 1:length(IBP)
    %The respective QRS peak is picked.
    ECGpeak=IBP(ii);
    %The limits are defined.
    bottommin = max(1,ECGpeak);
    if type == 2
        bottommin = max(1,floor(ECGpeak+kmin/8));
    end
    bottommax = max(1,ECGpeak);
    topmin = min(ECGpeak+kmin, length(ECG)-1);
    topmax = min(ECGpeak+kmax, length(ECG)-1);
    %The maximum and minimum of the pulse wave is found using the max
    %function inside the limits.
    peakIPG = max(Z(bottommax:topmax));
    peakIPG_index = find(Z(bottommax:topmax)==peakIPG);
    peakIPG_index = peakIPG_index + bottommax;

    lowIPG = min(Z(bottommin:topmin));
    lowIPG_index = find(Z(bottommin:topmin)==lowIPG);
    lowIPG_index = lowIPG_index + bottommin;
    %The new maxima and minima are stored.
    IPGmax=[IPGmax,peakIPG];
    IPGmin=[IPGmin,lowIPG];
end

```

```
%The index vectors are updated. In case consecutive points present
the %same amplitude, the middle one will be picked.
IPGmax_index=[IPGmax_index,peakIPG_index(ceil(length(peakIPG_index)/2)
)];
IPGmin_index=[IPGmin_index,lowIPG_index(ceil(length(lowIPG_index)/2))]
;
end
end
```

A.3 Impedance First Derivative Characterization

```
function[dZ_min,dZ_mini,dZ_X,dZ_Xi,dZ_max,dZ_maxi,tejec,dZmax,incZ] =
characterizationdZ(ECG,Z,type,fs)

Fn = fs/2; % Nyquist Frequency (Hz)
Wp = [0.5 40.0]/Fn; % Passband Frequencies (Normalised)
Ws = [0.4 40.1]/Fn; % Stopband Frequencies (Normalised)
Rp = 10; % Passband Ripple (dB)
Rs = 50; % Stopband Ripple (dB)
[n,Ws] = cheb2ord(Wp,Ws,Rp,Rs); % Filter Order
[z,p,k] = cheby2(n,Rs,Ws); % Filter Design
% Convert To Second-Order-Section For Stability
[sosbp,gbp] = zp2sos(z,p,k);
tv = linspace(0, 1, length(Z))/fs; % Time Vector (s)
Z = filtfilt(sosbp,gbp, Z);
dZ = fs*(diff(Z));
% The maxima and minima of the IPG signal are found calling the
characterization function.
[IBP,IPGmax, IPGmin,
IPGmax_index,IPGmin_index]=characterization(ECG,Z,type,fs);
% The B points are found taking the indexes of the minima from the IPG
signals and taking the associated points in the first derivative.
dZ_min = dZ(IPGmin_index); dZ_mini=[]; int=200;

%Void vectors are generated to store the data.
dZ_maxi = []; dZ_max=[]; dZ_Xi = []; dZ_X = [];
x = [1:length(Z)]/fs;
%A loop is started for each minimum of the IPG signal.
for i = 1:length(IPGmin_index)
    %The limits will be set using the indexes of the corresponding
    %maximum and minimum of the pulse wave to find the E points.
    bottom = IPGmin_index(i);
    top = IPGmax_index(i);
    %Some conditions are imposed to assure the limits are correct.
    if bottom>top && (i+1)<length(IPGmax_index)
        top = IPGmax_index(i+1);
    elseif bottom>top && (i+1)>length(IPGmax_index)
        top = length(dZ);
    elseif top > length(dZ)
        top = length(dZ)
    end
    %The E points are found using the indexes of the corresponding
    %minimum and maximum.
    peak = max(dZ(bottom:top));
    peak_index = find(dZ(bottom:top)==peak);
    peak_index = peak_index + bottom;
    dZ_max = [dZ_max,peak(ceil(length(peak)/2))];
    dZ_maxi=[dZ_maxi , peak_index(ceil(length(peak)/2))];
```

```

%Now the minima of the derivative signal are found
%The new limits used to find the X points will be defined. The
%bottom limit will be the predecessor E points. For the
%upper limit 400 will be added to the lower limit index.
bottom = dZ_maxi(end);
top = min(bottom + 400,length(dZ));
%The X point amplitude and index is found using the min.
low = min(dZ(bottom:top));
low_index = find(dZ(bottom:top)==low);
low_index = low_index + bottom;
%The corresponding vectors are updated, storing the the newfound
%values. Just in case some consecutive points present the same
%amplitude, the middle point will be picked.
dZ_X = [dZ_X,low(ceil(length(low)/2))];
dZ_Xi=[dZ_Xi , low_index(ceil(length(low_index)/2))];
end

%In the case the analogical derivative is used, the B points need to
%be set to zero, as most of them do not correspond to zero.
%A loop is generated for each B point in the vector.
for j = 1:length(dZ_min)
    %As the real zero will be close to the current index, a inspection
    %in the last 100 samples will be done.
    bottom = dZ_maxi(j)-220;
    top = dZ_maxi(j);
    %The new minimum of the zone is found, that will correspond to the
    %closer point to zero.
    minimum = min(abs(dZ(bottom:top)));
    minimum_index =find(abs(dZ(bottom:top))==minimum);
    %In case some points present the same amplitude, the last one is
    %picked.
    if length(minimum_index)>1
        minimum_index=minimum_index(end);
    end
    %The B points storing vector is updated.
    minimum_index = minimum_index + bottom;
    minimum = dZ(minimum_index);
    dZ_min(j) = minimum;
    dZ_mini=[dZ_mini, minimum_index];
end

===== Final Parameters=====
=====t_ejec=====
%% The t_ejec variable is computed. To eliminate much bigger or that
%%smaller values, an average is performed and a loop will erase the
%% present big differences from the average.

tejecvec = (abs(dZ_mini-dZ_Xi))/fs;
tejec = mean(abs(dZ_mini-dZ_Xi))/fs;
ivec=[];
for i = 1:length(tejecvec)
    if tejecvec(i) > 2*tejec
        ivec = [ivec,i];
    end
end
tejecvec(ivec) = [];
tejec = mean(tejecvec);

```

```
=====dZ/dt_max=====
%% The same procedure as before is repeated.
dZmaxvec = (abs(dZ_max));
dZmax = mean(abs(dZ_max));
ivec=[];
for i = 1:length(dZmaxvec)
    if dZmaxvec(i) > 2*dZmax
        ivec = [ivec,i];
    end
end
dZmaxvec(ivec) = [];
dZmax = mean(dZminvec);

=====inc Z=====
%% The same procedure as before is repeated.
incZvec = (IPGmax-IPGmin);
incZ = mean(IPGmax-IPGmin);
ivec=[];
for i = 1:length(incZvec)
    if incZvec(i) > 2*incZ
        ivec = [ivec,i];
    end
end
incZvec(ivec) = [];
incZ = mean(incZvec);
```

A.4 Integration and Average Form

```
function[tej,meanmm,suma,I] = promig(ECG, Z, type, fs)
%% This code has as a result the average form of a signal
%(ICG/IPG/PPG) and the integration of a pulse wave.
%The impedance signal is characterized using the corresponding code.
[IBP,IPGmax, IPGmin,
IPGmax_index,IPGmin_index]=characterization(ECG,Z,type,fs);
%An integration vector is created to store the integration of each
%pulse wave. A matrix is generated to store pulse wave form.
Ivec = [];
mat = zeros(10000,100);
%The average minimum to minimum distance is computed
meanmm = mean(diff(IPGmin_index)); meanmm = floor(meanmm);
%The mean time between the minima of the impedance signal and the ECG
peaks is computed, thus knowing the delay.
tej = mean(abs(IBP-IPGmin_index))/fs; count = 0;
%A loop is generated. For each minimum, take the corresponding pulse
%wave.
for i=1:length(IPGmin)-1
    xmin = IPGmin_index(i); %The minimum index is selected.
    xmax = IPGmin_index(i+1); %The maximum index is selected.
    %A condition is imposed to assure no pulse wave is lost.
    if abs(xmin-xmax) < 1.5*meanmm && abs(xmin-xmax)>0.5*meanmm
        %A temporary variable is created to store the pulse wave form.
        Z_temp = Z(xmin:xmax);
        %The minimum of the pulse wave is set to zero.
        Z_temp = Z_temp - min(Z_temp);
        %Only the pulse waves wider than the mean width will be stored.
        if length(Z_temp)>meanmm
            count = count + 1;
            mat(i,1:length(Z_temp))=Z_temp;
        end
        %The integration of all pulse wave is computed using the trapz()
        %matlab function.
        I = trapz([1:length(Z_temp)]/fs,Z_temp);
        Ivec = [Ivec, I];
    end
end
%A new variable is created to sum all pulse wave form and compute the
%average.
suma = 0;
for i=1:100
    suma = suma + mat(i,:);
end
%The suma variable is divided by the number of wave pulses that have
%been summed.
suma = suma/count;
%The mean integration is computed.
I = sum(Ivec)/length(Ivec);
end
```

A.4 Obtention of times (minima-peaks and maxima-peaks) and slope.

```

datavec=[]; datavecejec=[]; idatavec=[1:9]; idatavecejec=[1:9];
%%=====Z1=====
%% Z1 The first measure of the subject is uploaded.
load('Z1.mat'); fs=2000; ECG = data(:,3); PPG = data(:,4);
%The impedance signal is inversed.
Z = -data(:,1); type = 1;
%The impedance signal is filtered and the derivative is obtained.
[Z,dZ]=filtering(Z); Z1 = Z;
%The impedance signal is characterized.
[IBP,IPGmax1, IPGmin1,
IPGmax_index1,IPGmin_index1]=characterization4_0(ECG,Z,type,fs);
%The mean slope is computed.
der1 = (IPGmax1-IPGmin1)./((IPGmax_index1-IPGmin_index1));
mder1 = sum(der1)/length(der1);
%The mean time between minima and the ECG peaks is computed.
tdiffmax1 = abs(IBP-IPGmax_index1);
Tdiffmean = mean(tdiffmax1(2:end-1))/fs;
datavec = [datavec, Tdiffmean];
%The time between maxima and ECG peaks is computed
tdiffmin1 = abs(IBP-IPGmin_index1);
Tdiffmean = mean(tdiffmin1(2:end-1))/fs;
datavecejec = [datavecejec, Tdiffmean];

%The same procedure is repeated for PPG and the rest of IPG signals.

%%=====PPG(Z6)=====
%% PPG
load('Z3.mat'); fs=2000; PPG = data(:,4); ECG = data(:,3);
Z = -data(:,1); type = 2;
[PPG,dZ]=filtering(PPG); ZPPG = PPG;
[IBP,IPGmaxPPG, IPGminPPG,
IPGmax_indexPPG,IPGmin_indexPPG]=characterization4_0(ECG, PPG,type,
fs);
derPPG = (IPGmaxPPG-IPGminPPG)./((IPGmax_indexPPG-IPGmin_indexPPG));
mderPPG = sum(derPPG)/length(derPPG);
tdiffmaxPPG = abs(IBP-IPGmax_indexPPG);
TdiffmeanPPG = mean(tdiffmaxPPG(2:end-1))/fs;
tdiffminPPG = abs(IBP-IPGmin_indexPPG);
TdiffmeanejecPPG = mean(tdiffminPPG(2:end-1))/fs;

%%=====Z2=====
%% Z2
load('Z2.mat'); fs=2000; Z2i = data(:,1); ECG = data(:,3);
Z = -data(:,1); type = 1;
[Z,dZ]=filtering(Z); Z2 = Z;
[IBP,IPGmax2, IPGmin2,
IPGmax_index2,IPGmin_index2]=characterization4_0(ECG,Z,type,fs);
der2 = (IPGmax2-IPGmin2)./((IPGmax_index2-IPGmin_index2)); mder2 =
sum(der2)/length(der2);
tdiffmax2 = abs(IBP-IPGmax_index2);
Tdiffmean = mean(tdiffmax2(2:end-1))/fs;
datavec = [datavec, Tdiffmean];
tdiffmin2 = abs(IBP-IPGmin_index2);

```

```

Tdiffmean = mean(tdiffmin2(2:end-1))/fs; datavecejec = [datavecejec,
Tdiffmean];
%%=====Z3=====
%% Z3
load('Z3.mat'); fs=2000; Z3i = data(:,1); ECG = data(:,3);
Z = -data(:,1); type = 2;
[Z,dZ]=filtering(Z); Z3 = Z;
[IBP,IPGmax3, IPGmin3,
IPGmax_index3,IPGmin_index3]=characterization4_0(ECG,Z,type,fs);
tdiffmax3 = abs(IBP-IPGmax_index3);
Tdiffmean = mean(tdiffmax3(2:end-1))/fs;
datavec = [datavec, Tdiffmean];
der3 = (IPGmax3-IPGmin3)./((IPGmax_index3-IPGmin_index3));
mder3 = sum(der3)/length(der3);
tdiffmin3 = abs(IBP-IPGmin_index3);
Tdiffmean = mean(tdiffmin3(2:end-1))/fs;
datavecejec = [datavecejec, Tdiffmean];

%%=====Z4=====
%% Z4
load('Z4.mat'); fs=2000; Z4i = data(:,1);ECG = data(:,3);
Z = -data(:,1); type = 2;
[Z,dZ]=filtering(Z); Z4 = Z;
[IBP,IPGmax4, IPGmin4,
IPGmax_index4,IPGmin_index4]=characterization4_0(ECG,Z,type,fs);
tdiffmax4 = abs(IBP-IPGmax_index4);
Tdiffmean = mean(tdiffmax4(2:end-1))/fs;
datavec = [datavec, Tdiffmean];
der4 = (IPGmax4-IPGmin4)./((IPGmax_index4-IPGmin_index4));
mder4 = sum(der4)/length(der4);
tdiffmin4 = abs(IBP-IPGmin_index4);
Tdiffmean = mean(tdiffmin4(2:end-1))/fs; datavecejec = [datavecejec,
Tdiffmean];

%%=====Z5=====
%% Z5
load('Z5.mat'); fs=2000; Z5i = data(:,1); ECG = data(:,3);
Z = -data(:,1); type = 2;
[Z,dZ]=filtering(Z); Z5 = Z;
[IBP,IPGmax5, IPGmin5,
IPGmax_index5,IPGmin_index5]=characterization4_0(ECG,Z,type,fs);
tdiffmax5 = abs(IBP-IPGmax_index5);
Tdiffmean = mean(tdiffmax5(2:end-1))/fs;
datavec = [datavec, Tdiffmean];
%bestfit = abs(tdiff/fs-Tdiffmean); [value,index] = min(bestfit);
der5 = (IPGmax5-IPGmin5)./((IPGmax_index5-IPGmin_index5));
mder5 = sum(der5)/length(der5);
tdiffmin5 = abs(IBP-IPGmin_index5);
Tdiffmean = mean(tdiffmin5(2:end-1))/fs; d
atavecejec = [datavecejec, Tdiffmean];

%% The PPG time values are added in the vector in the sixth position.
datavec = [datavec, TdiffmeanPPG];
datavecejec = [datavecejec, TdiffmeanejecPPG];

```



```

%%=====Z7=====
%% Z7
load('Z7.mat'); fs=2000; ECG = data(:,3); Z = -data(:,1); type = 3;
[Z,dZ]=filtering(Z); Z7 = Z;
[IBP,IPGmax7, IPGmin7,
IPGmax_index7,IPGmin_index7]=characterization4_0(ECG,Z,type,fs);
tdiffmax7 = abs(IBP-IPGmax_index7);
Tdiffmean = mean(tdiffmax7(2:end-1))/fs;
datavec = [datavec, Tdiffmean];
%bestfit = abs(tdiff/fs-Tdiffmean); [value,index] = min(bestfit);
der7 = (IPGmax7-IPGmin7)./((IPGmax_index7-IPGmin_index7));
mder7 = sum(der7)/length(der7);
tdiffmin7 = abs(IBP-IPGmin_index7);
Tdiffmean = mean(tdiffmin7(2:end-1))/fs;
datavecejec = [datavecejec, Tdiffmean];

%%=====Z8=====
%% Z8
load('Z8.mat'); fs=2000; ECG = data(:,3); Z = -data(:,1); type = 3;
[Z,dZ]=filtering(Z); Z8 = Z;
[IBP,IPGmax8, IPGmin8,
IPGmax_index8,IPGmin_index8]=characterization4_0(ECG,Z,type,fs);
tdiffmax8 = abs(IBP-IPGmax_index8);
Tdiffmean = mean(tdiffmax8(2:end-1))/fs;
datavec = [datavec, Tdiffmean];
der8 = (IPGmax8-IPGmin8)./((IPGmax_index8-IPGmin_index8));
mder8 = sum(der8)/length(der8);
tdiffmin8 = abs(IBP-IPGmin_index8);
Tdiffmean = mean(tdiffmin8(2:end-1))/fs;
datavecejec = [datavecejec, Tdiffmean];

%%=====Z9=====
%% Z9
load('Z9.mat'); fs=2000; ECG = data(:,3);
Z = -data(:,1); type = 3;
[Z,dZ]=filtering(Z); Z9 = Z;
[IBP,IPGmax9, IPGmin9,
IPGmax_index9,IPGmin_index9]=characterization4_0(ECG,Z,type,fs);
tdiffmax9 = abs(IBP-IPGmax_index9);
Tdiffmean = mean(tdiffmax9(2:end-1))/fs;
datavec = [datavec, Tdiffmean];
der9 = (IPGmax9-IPGmin9)./((IPGmax_index9-IPGmin_index9));
mder9 = sum(der9)/length(der9);
tdiffmin9 = abs(IBP-IPGmin_index9);
Tdiffmean = mean(tdiffmin9(2:end-1))/fs;
datavecejec = [datavecejec, Tdiffmean];

%% A vector containing each slope is created with the correct order.
der = [mder1,mder2,mder3,mder4,mder5,mderPPG,mder7,mder8,mder9];

```

A.5. Stroke Volume Obtention

```
function[SV]=SVfun(Z, ECG, type, fs,Z0,W)
%The impedance signals is filtered and the first derivative is
%computed.
[Z,dZ]=filtering(Z);
%The impedance first derivative is characterized.
function[dZ_min,dZ_mini,dZ_X,dZ_Xi,dZ_max,dZ_maxi,tejec,dZmax,incZ] =
characterizationdZ(ECG,Z,type,fs);
SV = 32*W^1.02*(dZmax/Z0)^(0.5).*abs(tejec);
end
```

Appendix B

TABLES OF PARAMETERS FOR EACH SUBJECT

SUBJECT 1				
Signal	QRS-min [ms]	QRS - max [ms]	Slope (x1000)	Integration ($\times f_s$)
Z1	90.12	250.50	0.8798	214.12
Z2	88.54	246.12	0.6093	155.79
Z3	164.96	276.15	0.0779	17.79
Z4	167.47	280.12	0.0525	11.16
Z5	164.19	284.19	0.0285	10.53
Z6(PPG)	198.70	386.55	2.625	788.24
Z7	94.80	282.05	0.375	150.52
Z8	139.00	317.89	0.1157	33.35
Z9	110.62	297.12	0.3987	170.41

Table 12. Parameters of the Subject 1.

SUBJECT 2				
Signal	QRS-min [ms]	QRS - max [ms]	Slope (x1000)	Integration ($\times f_s$)
Z1	77.50	221.25	0.4812	107.61
Z2	78.85	244.51	0.5168	141.05
Z3	144.92	279.79	0.1967	40.66
Z4	155.22	286.65	0.1015	18.94
Z5	155.82	288.85	0.0378	13.808
Z6 (PPG)	159.80	361.46	3.678	1022.42
Z7	122.11	270.47	0.5877	259.14
Z8	153.45	328.69	0.3001	89.581
Z9	120.6	308.12	0.4402	163.41

Table 13. Parameters of the Subject 2.

SUBJECT 3				
Signal	QRS-min [ms]	QRS - max [ms]	Slope (x1000)	Integration ($\times f_s$)
Z1	44.46	244.86	0.3232	155.20
Z2	65.20	268.12	0.2851	111.83
Z3	140.69	290.12	0.1204	53.45
Z4	153.18	300.81	0.0875	32.22
Z5	181.21	291.83	0.0396	10.29
Z6 (PPG)	183.66	338.12	0.8919	444.22
Z7	84.31	284.11	0.6132	245.85
Z8	161.23	347.79	0.2548	78.92
Z9	114.94	339.68	0.2466	104.6

Table 14. Parameters of the Subject 3.

SUBJECT 4				
Signal	QRS-min [ms]	QRS-max [ms]	Slope ($\times 1000$)	Integration ($\times f_s$)
Z1	102.83	258.55	0.6438	155.21
Z2	97.71	275.79	0.4396	106.19
Z3	128.99	299.09	0.1814	55.39
Z4	146.71	317.88	0.1323	38.37
Z5	136.27	278.93	0.0579	12.52
Z6(PPG)	166.86	327.90	7.4767	806.93
Z7	41.19	336.52	0.5861	356.70
Z8	157.04	342.34	0.1806	68.33
Z9	156.62	337.95	0.2711	79.40

Table 15. Parameters of the Subject 4

SUBJECT 5				
Signal	QRS-min [ms]	QRS-max [ms]	Slope ($\times 1000$)	Integration ($\times f_s$)
Z1	31.49	245.89	0.2109	116.45
Z2	93.15	275.83	0.2892	162.61
Z3	173.59	268.0	0.1428	78.95
Z4	167.12	256.83	0.073	17.65
Z5	160.12	274.65	0.0368	13.37
Z6(PPG)	190.75	416.23	2.0207	1300
Z7	68.61	263.13	0.4101	422.27
Z8	134.01	302.84	0.1949	185.73
Z9	88.82	304.86	0.3222	123.40

Table 16. Parameters of the Subject 5

SUBJECT 6				
Signal	QRS-min [ms]	QRS - max [ms]	Slope (x1000)	Integration (x f_s)
Z1	66.50	292.73	0.3758	142.28
Z2	55.37	265.22	0.2810	87.83
Z3	196.88	269.70	0.1022	30.88
Z4	191.36	316.66	0.0387	13.68
Z5	181.17	271.00	0.0577	8.87
Z6(PPG)	177.14	364.91	2.2736	921.75
Z7	75.30	260.63	0.4827	136.61
Z8	155.52	323.77	0.3611	74.19
Z9	97.66	309.00	0.2826	87.91

Table 17. Parameters of the Subject 6.

SUBJECT 7				
Signal	QRS-min [ms]	QRS - max [ms]	Slope (x1000)	Integration (x f_s)
Z1	70.64	229.70	0.8067	201.74
Z2	66.36	240.45	0.6304	148.63
Z3	157.88	257.50	0.1666	32.12
Z4	153.41	257.56	0.0931	21.50
Z5	162.95	264.21	0.0746	22.22
Z6(PPG)	196.36	328.63	2.3486	160.19
Z7	80.55	249.51	0.7862	146.33
Z8	134.30	296.80	0.3863	68.70
Z9	85.25	290.18	0.3386	107.08

Table 18. Parameters of the Subject 7.

SUBJECT 8				
Signal	QRS-min [ms]	QRS - max [ms]	Slope ($\times 1000$)	Integration ($\times f_s$)
Z1	11.78	233.95	0.3709	120.91
Z2	11.04	266.39	0.2257	73.66
Z3	128.30	264.15	0.1538	29.14
Z4	140.37	275.51	0.0704	12.36
Z5	139.25	281.91	0.0550	8.39
Z6(PPG)	205.80	349.36	1.9167	394.48
Z7	68.75	264.95	0.3720	78.43
Z8	204.80	344.41	0.2791	73.06
Z9	135.36	331.10	0.2038	70.08

Table 19. Parameters of the Subject 8.

SUBJECT 9				
Signal	QRS-min [ms]	QRS - max [ms]	Slope ($\times 1000$)	Integration ($\times f_s$)
Z1	72.91	236.61	0.8094	154.82
Z2	68.21	247.71	0.6193	105.05
Z3	189.95	262.95	0.1665	41.39
Z4	180.52	261.75	0.0917	21.71
Z5	187.39	290.52	0.07340	14.69
Z6(PPG)	197.5	325.02	2.3568	1762.45
Z7	97.51	242.86	0.7920	162.61
Z8	163.33	291.87	0.3875	86.90
Z9	101.17	304.52	0.3451	90.20

Table 20. Parameters of the Subject 8.

SUBJECT 10				
Signal	QRS-min [ms]	QRS - max [ms]	Slope ($\times 1000$)	Integration ($\times f_s$)
Z1	28.91	224.42	0.5456	201.72
Z2	49.70	253.7	0.3610	148.63
Z3	129.86	268.45	0.1853	32.12
Z4	134.82	306.32	0.0942	21.50
Z5	152.98	271.11	0.0172	20.22
Z6(PPG)	176.25	343.33	3.3840	160.19
Z7	92.33	302.29	0.5085	146.33
Z8	159.45	351.73	0.1828	68.70
Z9	98.29	299.75	0.249	107.87

Table 21. Parameters of the Subject 10.

SUBJECT 11				
Signal	QRS-min [ms]	QRS - max [ms]	Slope ($\times 1000$)	Integration ($\times f_s$)
Z1	42.07	260.57	0.3879	109.87
Z2	70.96	244.88	0.3917	100.33
Z3	129.10	268.58	0.2038	51.96
Z4	160.21	258.52	0.0803	15.87
Z5	151.45	263.54	0.054	10.56
Z6(PPG)	166.52	316.15	1.4139	435.20
Z7	102.28	224.27	0.3983	79.92
Z8	62.29	277.64	0.1737	52.93
Z9	142.32	322.80	0.1370	29.14

Table 22. Parameters of the Subject 11.

Appendix C

HARDWARE CIRCUITS DESIGN

C.1 ECG

C.1.1 ECG Schema

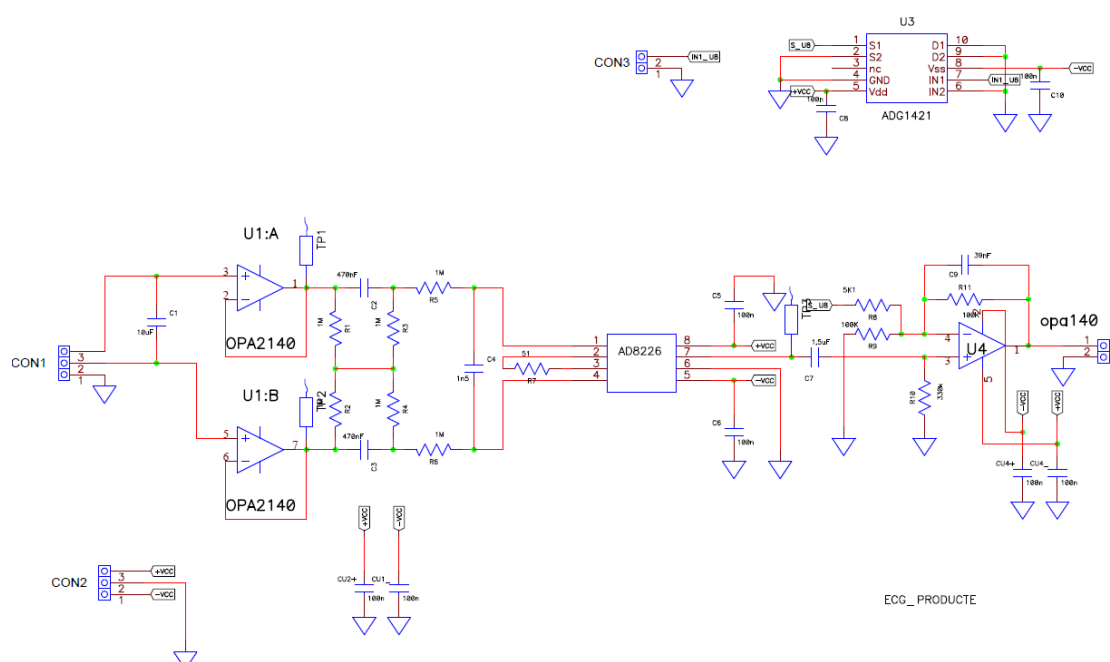


Figure C.1. ECG circuit schema design.

C.1.2 ECG Board

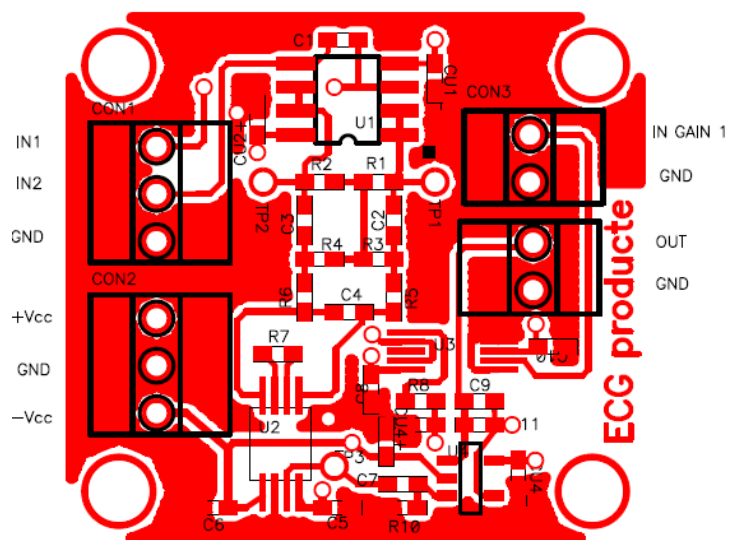


Figure C.2. Frontal ECG board.

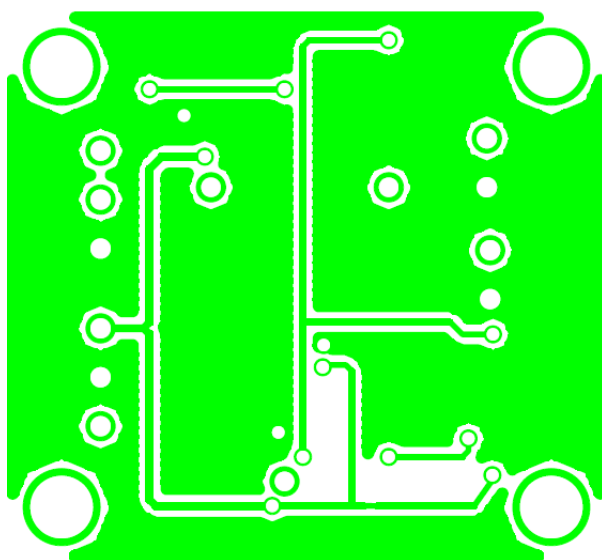


Figure C.3. Rear ECG board.

C.2. IPG

C.2.1 IPG Schema

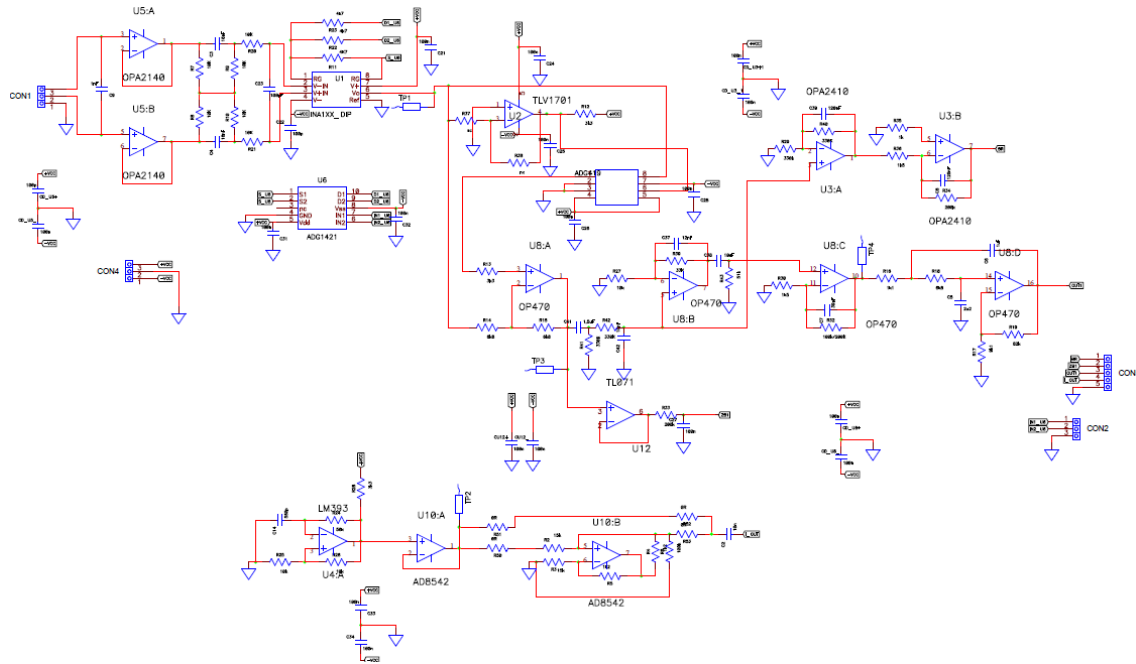


Figure C.4. IPG circuit schema design

C.2.2 ECG Board

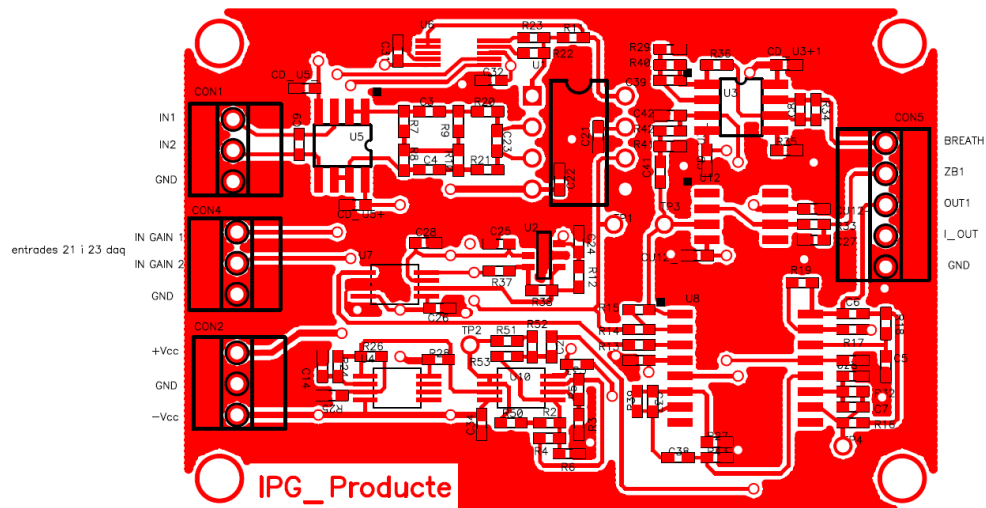


Figure C.5. Frontal IPG board.

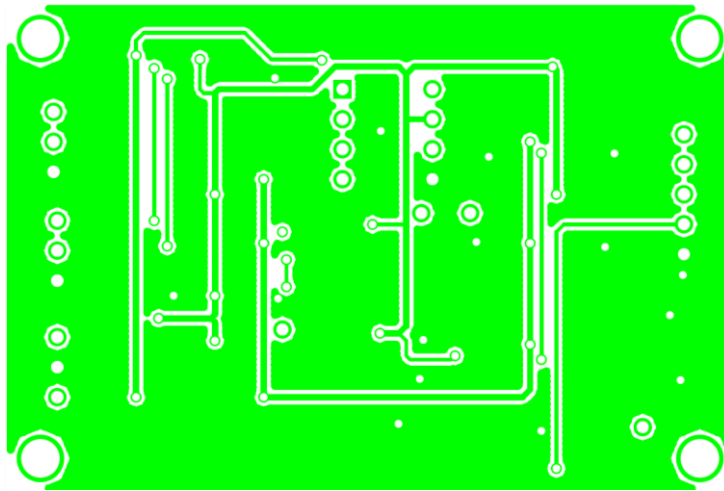


Figure C.6. Rear IPG board.

C.3. PPG

C.3.1 PPG Schema

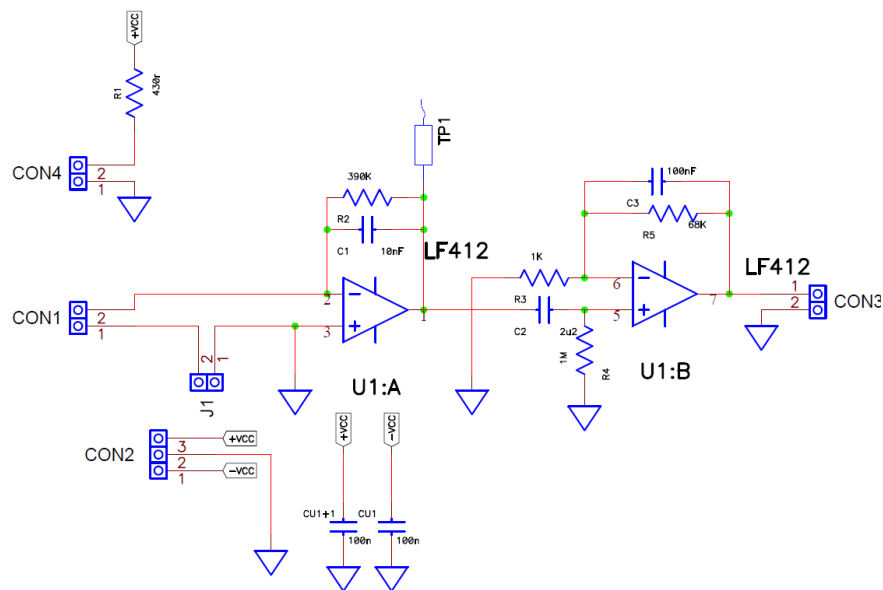


Figure C.7. PPG circuit schema design.

C.3.2 PPG Board

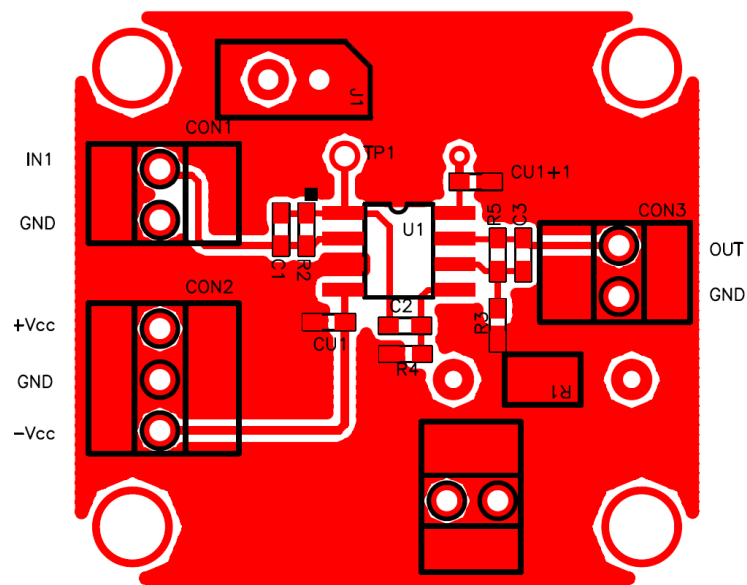


Figure C.8. Frontal PPG board.

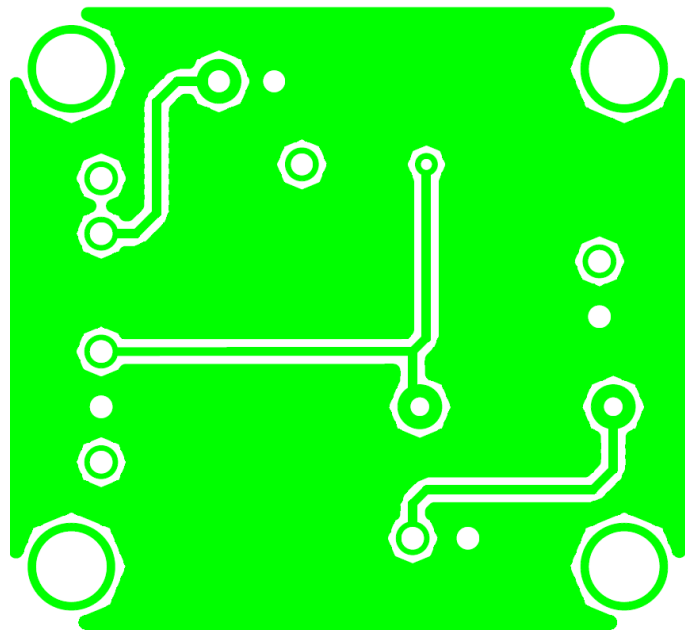


Figure C.9. Rear PPG board.

Bibliography

- [1] World Health Organization (WHO), "Cardiovascular Diseases," [Online]. Available: https://www.who.int/cardiovascular_diseases/en/.
- [2] Allen J., "Photoplethysmography and its application in clinical physiological measurement," *Physiological Measurement*, vol. 28, no. R1-R39, 2007.
- [3] Lee S.P., Grace H., Wright D.E. and *et al.*, "Highly flexible, wearable, and disposable cardiac biosensors for remote and ambulatory monitoring," *Digital Medicine* volume, no. 2, 2018.
- [4] Yasbanoo M., Raghadd A., Duero J.P. and *et al.*, "Assessing the Use of Wrist-Worn Devices in Patients With Heart Failure: Feasibility Study," *JMIR Cardio*, vol. 1, no. 2, 2017.
- [5] J Jungdon L., Jeon B., Jaehon C. and *et al.*, "Design and Implementation of a Wearable ECG System," *Internation Journal of Smart Home*, vol. 7, no. 2, 2013.
- [6] Garcia O.A., Perez J.A., Luna P.S., and *et al.*, "Impedance Plethysmography Detection with Mobile and Concealed Devices," *IEEE LATIN AMERICA TRANSACTIONS*, vol. 14, no. 4, 2016.
- [7] Nyboer J. and Bango S., "Electrical impedance changes of the heart in relation to electrocardiograms and heart sounds.," *Radiocardiograms*, 1940.
- [8] Kubiceck W.G, Karneigs J.N. and *et al.*, "Development and evaluation of an impedance cardiac output system," *Aerosp. Med.*, 1966.
- [9] Murray W. and Foster P. and *et al.*, "The peripheral pulse wave: information overlooked.," *Journal of Clinical Monitoring and Computing.*, 1996.

- [10] Daimiwal N., Sundharajan M. and *et al.*, "Non Invasive Measurement and Analysis of Cardiac," *International Journal of Computer Applications* , 2016.
- [11] Bernstein D.P, Henry I.C., Lemmens H.J. and *et al.*, "Validation of stroke volume and cardiac output by electrical interrogation of the brachial artery in normals: assesment of strenghts, limitations and source of error.," *J Clin Monit Comput*, 2015.
- [12] Wang J.J., Kao T. and Hu W.C. and *et al.*, "On Measuring the Changes in Stroke Volume from a peripheral artery by means of electrical impedance plethysmography."
- [13] Thibodeau G.A and Patton K.T., *Anatomy and Physiology*, Harcourt, 2000.
- [14] Choudari P. and Panse M.S., "Measurement of Cardiac Output using Bioimpedance Method," *International Journal of Computer Applications* , no. 0975 – 8887, 2013.
- [15] Bighamian R., Hahn J.O and *et al.*, "Relationship between Stroke Volume and Pulse Pressure during Blood Volume Perturbation.," *Hindawi Publishing Corporation*, 2014.
- [16] Keerthi G.R., Vijaya P.A. and *et al.*, "ECG Signal Characterization and Correlation To Heart Abnormalities," *International Research Journal of Engineering and Technology (IRJET)*, 2017.
- [17] Lamberts R., Visser K.R. and Zijlstra W.G., *Impedance Cardiography*, 1984.
- [18] Cybulski G., *Ambulatory Impedance Cardiography: The systems and their applications*, Springer, 2011.
- [19] M. Elgendi, "On the Analysis of Fingertip Photoplethysmogram Signals," *Current Cardiology Reviews*, vol. 8, pp. 14-25, 2012.
- [20] Bernstein D.P., Henry I.C., Banet M.J. and *et al.*, "Stroke volume obtained by electrical interrogation of the brachial artery: transbrachial electrical bioimpedance velocimetry," *Physiological Measurement* , 2012.

- [21] Bernstein D.P. and Lemmens H.J., "Impedance cardiography: development of the stroke volume equations and their electrodynamic and biophysical foundations," *Biomechanical Systems Technology*.
- [22] Biopac Systems. INC., "MP36 BIOPAC device specifications," [Online]. Available: <https://www.biopac.com/wp-content/uploads/MP36-MP45.pdf>.
- [23] Lin C.H., "Science Direct," *Science Direct*, 2007.
- [24] Jagtap P.S. and Jagtap R.R., "Electrocardiogram (ECG) Signal Analysis and Feature Extraction: A Survey," *International Journal of Computer Science* , 2015.
- [25] Pan J. and Tompkins W.J., "A Real-Time QRS Detection Algorithm," *IEEE TRANSACTIONS ON BIOMEDICAL ENGINEERING*, 1985.
- [26] "USB-1608FS-Plus Simultaneous USB DAQ Device," Measurement Computing, [Online]. Available: <https://www.mccdaq.com/PDFs/specs/DS-USB-1608FS-Plus.pdf>.
- [27] S.-7. Photosensor, "RS components," [Online]. Available: <https://docs-apac.rs-online.com/webdocs/1545/0900766b81545a51.pdf>.